THE UNIVERSITY OF CHICAGO
BIOLOGICAL SCIENCES

TIPP2017

Future Applications in Medical Imaging

Chin-Tu Chen, PhD

Department of Radiology and Committee on Medical Physics

Pritzker School of Medicine & Biological Sciences Division

The University of Chicago

Overview

- Limited & Select Examples
- TIPP Connections
- From History to Emerging Future
- Interactive Synergy
- Forward-Looking & Next-Generation
- Routine Practice & Wide-Spread Uses
- Less Technical Details
- More Medical Impacts

Outlines

- **Historic Perspectives: TIPP Impact on Medicine**
- **Mutual Benefits of TIPP & Medical Imaging (MI)**
- **Forward-Looking Applications: Challenges & Opportunities**
- **Summary**

75th Chicago Pile-1 (CP-1) Commemoration

Manhattan Project
December 2, 1942
Chicago Pile - One (CP1)

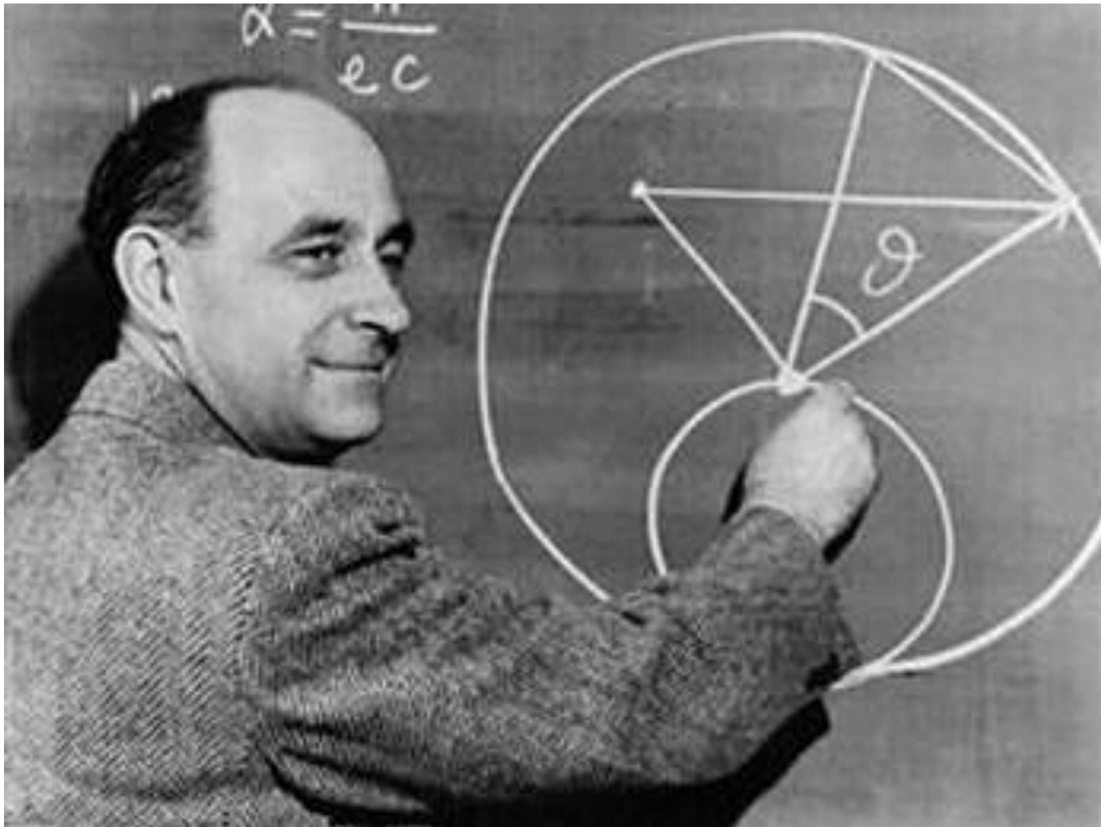

Enrico Fermi (1901-1954) received the 1938 Nobel Prize in Physics for his demonstrations of the existence of new radioactive elements produced by neutron irradiation, and for his related discovery of nuclear reactions brought about by slow neutrons.

On December 2, 1942
Man Achieved Here
The First Self-Sustaining
Chain Reaction
And Thereby
Initiated the
Controlled Release
of Nuclear Energy

Historic Evolution to Current Research

- *Post-WWII (1945)*
  "Atoms for Peace" Program
- *1953, Argonne Cancer Research Hospital (ACRH)*
  -- Peaceful Use of Atomic Energy in Medicine and Biology (Both Diagnosis & Therapy)
- *1974, Franklin McLean Memorial Research Institute (FMI)*
  -- PET/SPECT
- *2005, Functional & Molecular Imaging Core (FMI)*
  -- Expanded into CT, Ultrasound, Optical Imaging, Emerging Technologies, Multi-Modality

Quantitative & Integrative Multi-Modality Functional & Molecular Imaging (QIM-FMI)

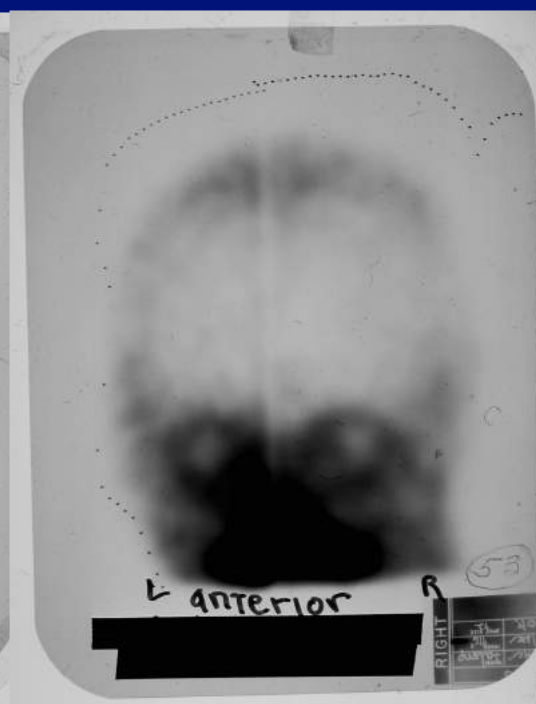

ACRH Brain Scanner, 1962

- *1962-63 The Birth of Modern Nuclear Medicine*

First Tc-99m Brain Scan
"First Molecular Image"

- *Multi-Disciplinary ACRH Molecular Imaging Team*

Paul Harper (Surgeon)
Robert Beck (Physicist)
Katherine Lathrop (Chemist)
Donald Charleston (Engineer)
Alex Gottschalk(Radiologist)

World's First Tc-99m Brain Image, 1963

New Disciplines at Interfaces of
Biology, Medicine, Physics, Chemistry, Mathematics, Computer/Computing Science, Material Science/Engineering, Electrical Engineering + X

Outlines

- **Historic Perspectives: TIPP Impact on Medicine**

TIPP & Medicine – Common Tech Platform

- **Diagnostic Imaging** - Radiation Detection
- **“Radiation” & “Particle” Therapy** - Accelerator
- ***“Thera[g]nostics”*** - **(Diagnostics + Therapeutics)** **i.e.,** Image-Guided Therapy

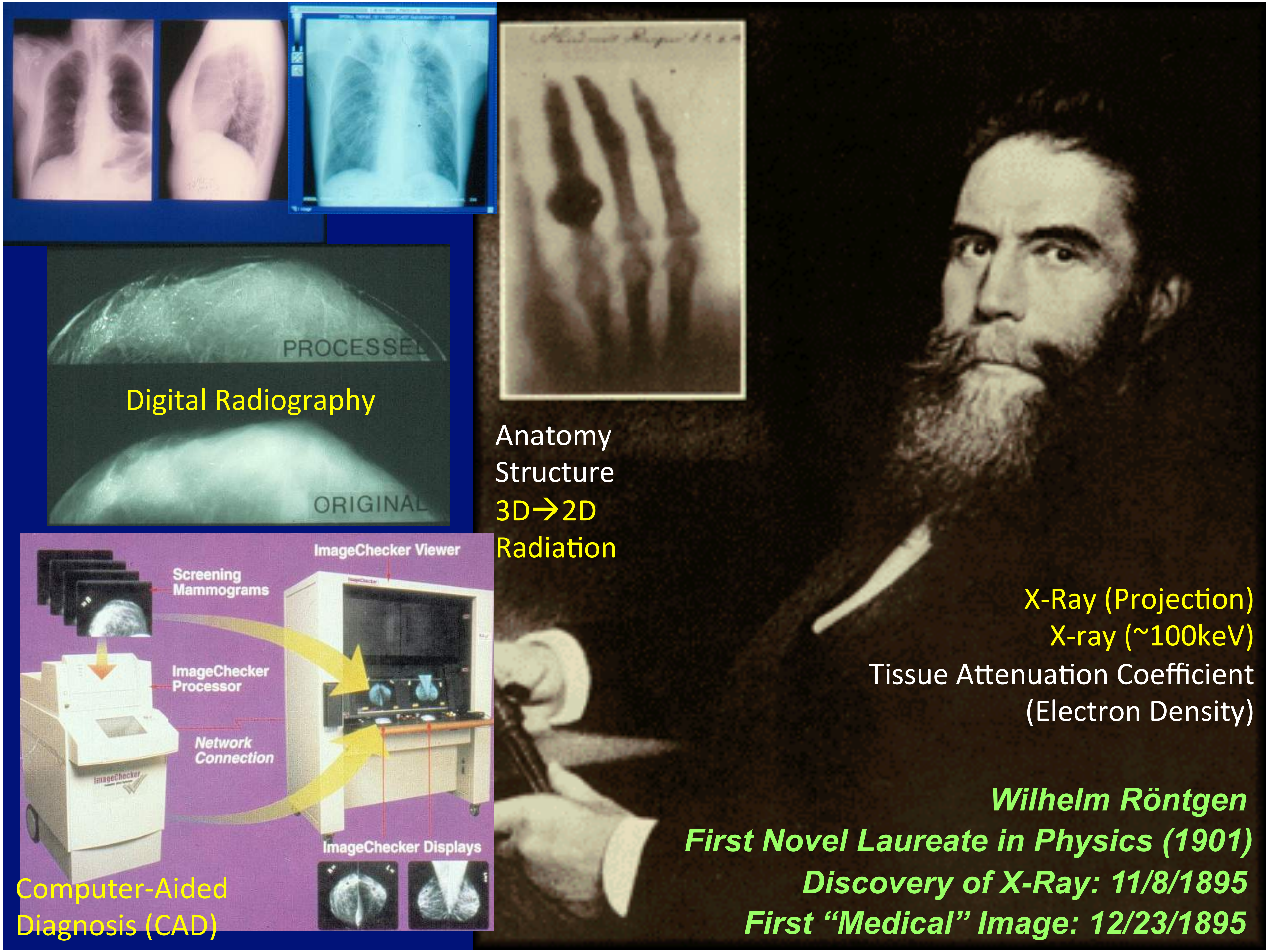
PROCESSED
Digital Radiography
ORIGINAL
ImageChecker Viewer
Screening Mammograms
ImageChecker Processor
Network Connection
ImageChecker Displays
Computer-Aided Diagnosis (CAD)
Anatomy
Structure
3D→2D
Radiation
X-Ray (Projection)
X-ray (~100keV)
Tissue Attenuation Coefficient
(Electron Density)
Wilhelm Röntgen
First Novel Laureate in Physics (1901)
Discovery of X-Ray: 11/8/1895
First "Medical" Image: 12/23/1895

X-Ray Computed Tomography (CT)

X-ray (~100keV)

Tissue Attenuation Coefficient

(Electron Density)

Anatomy & Structure

Multiple Slices in 3D, Radiation

Medical CT Images - Then and Now

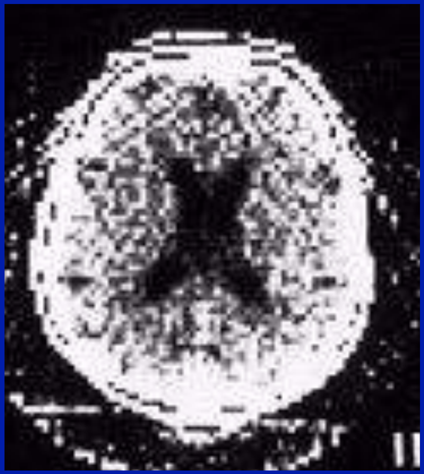

~1975

2001

Medical CT spatial resolution: < 1 mm

Micro CT spatial resolution: ~ 1-10 μm

Alan M. Cormack
(1924-1998)

Sir Godfrey N. Hounsfield
(1919-2004)

Alan M. Cormack and Sir Godfrey N. Hounsfield received the 1979 Nobel Prize in Physiology or Medicine for the development of computer assisted tomography (CT)

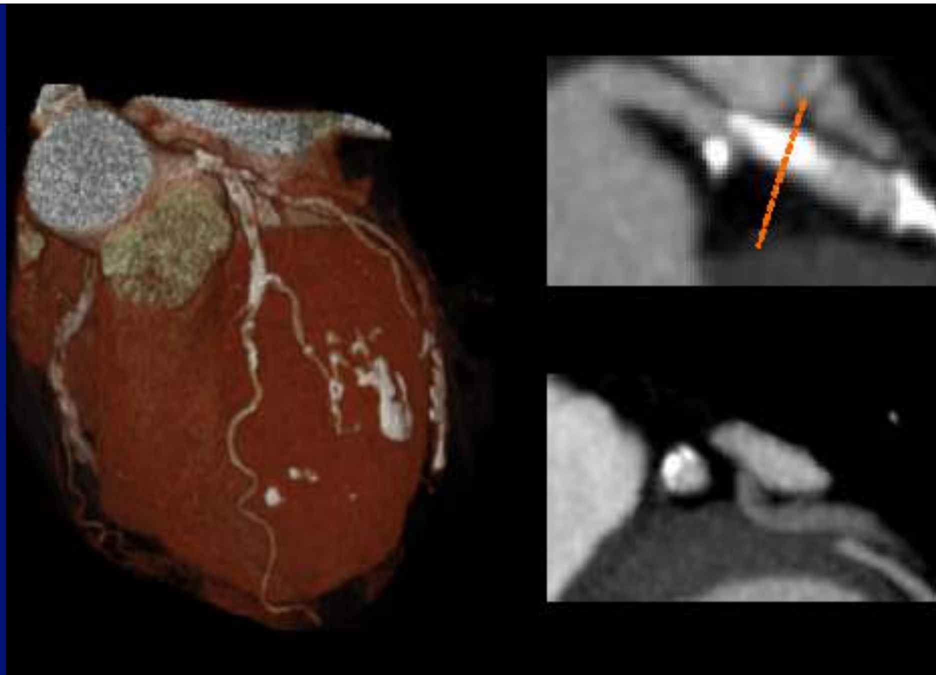

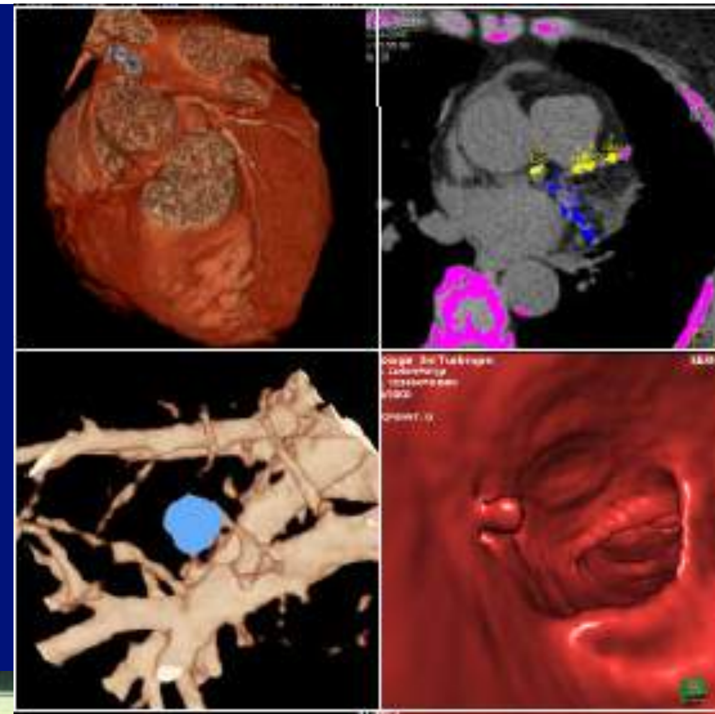

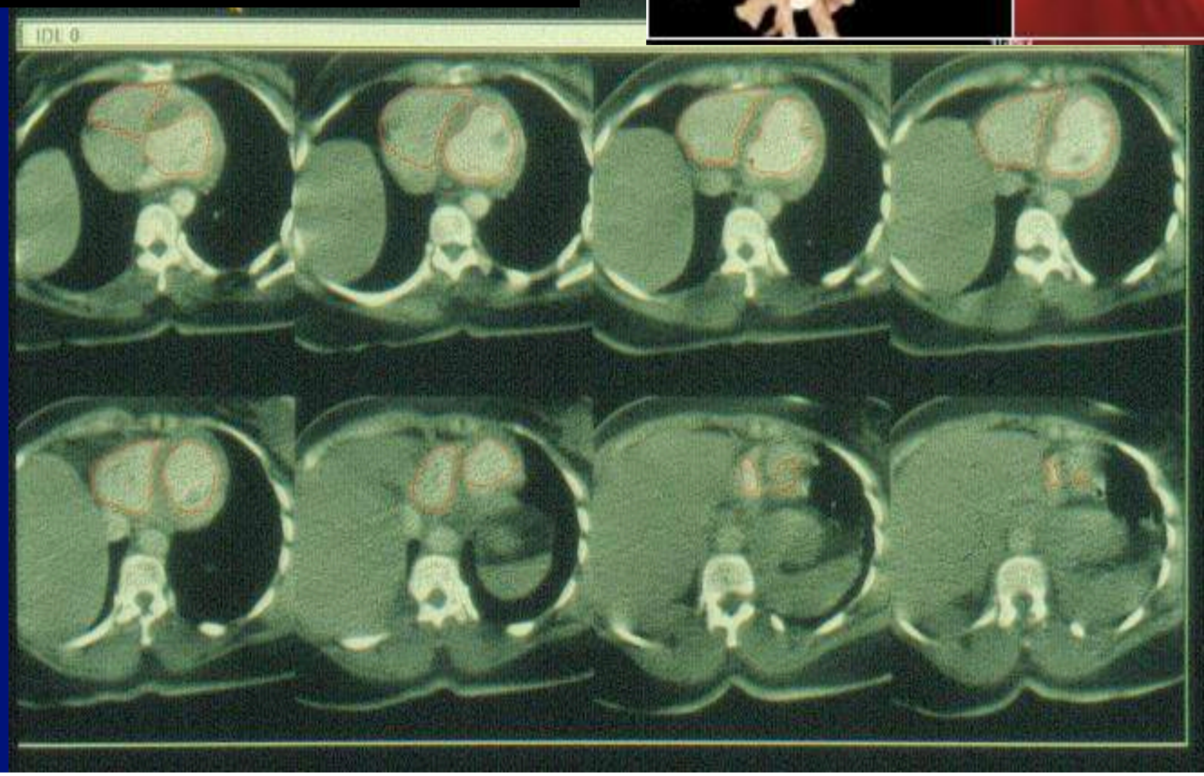

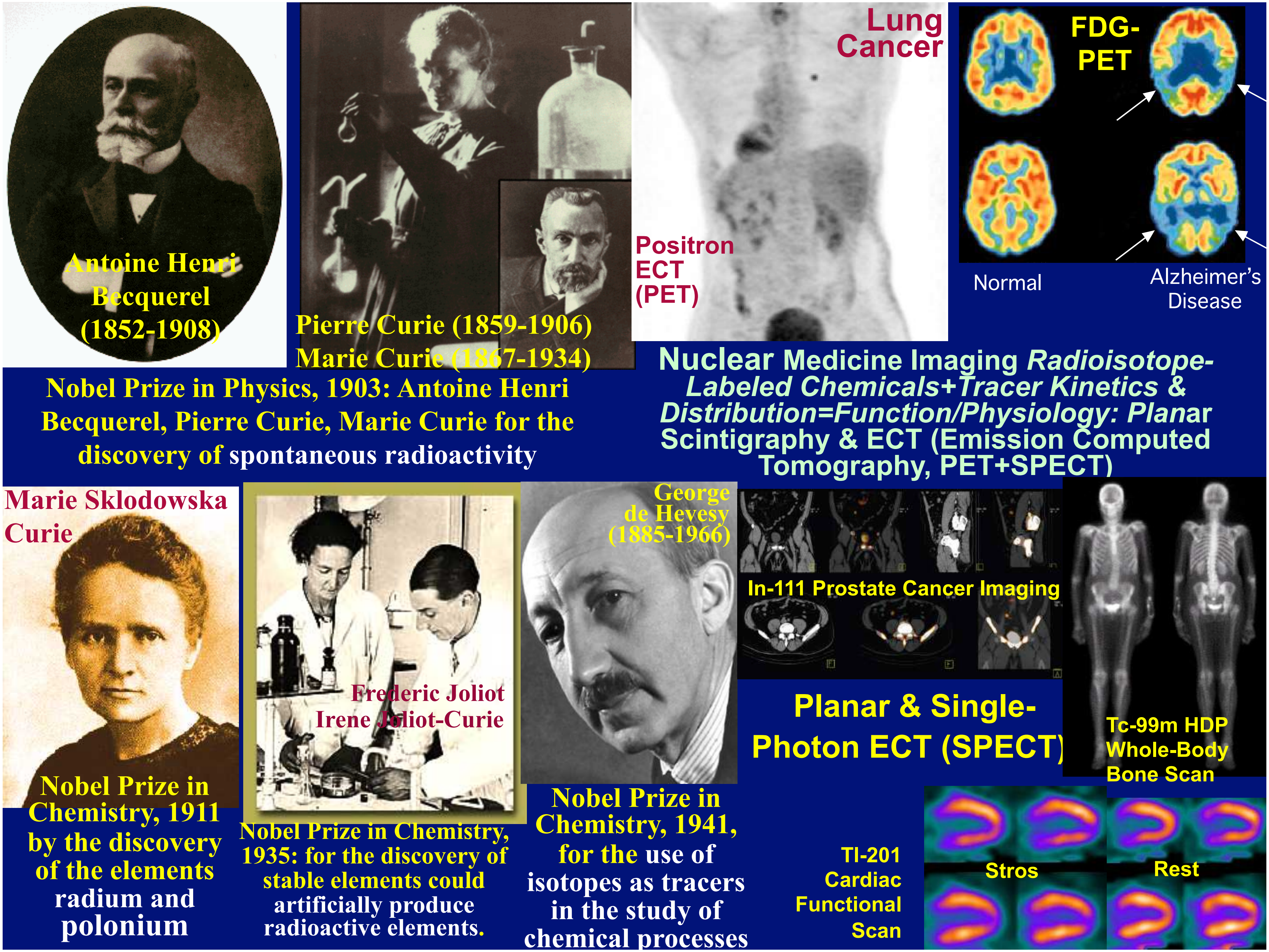

Antoine Henri Becquerel (1852-1908)
Pierre Curie (1859-1906)
Marie Curie (1867-1934)
Lung Cancer
Positron ECT (PET)
FDG-PET
Normal
Alzheimer's Disease
Nobel Prize in Physics, 1903: Antoine Henri Becquerel, Pierre Curie, Marie Curie for the discovery of spontaneous radioactivity
Nuclear Medicine Imaging Radioisotope-Labeled Chemicals+Tracer Kinetics & Distribution=Function/Physiology: Planar Scintigraphy & ECT (Emission Computed Tomography, PET+SPECT)
Marie Sklodowska Curie
Frederic Joliot
Irene Joliot-Curie
George de Hevesy (1885-1966)
In-111 Prostate Cancer Imaging
Planar & Single-Photon ECT (SPECT)
Tc-99m HDP Whole-Body Bone Scan
Nobel Prize in Chemistry, 1911 by the discovery of the elements radium and polonium
Nobel Prize in Chemistry, 1935: for the discovery of stable elements could artificially produce radioactive elements.
Nobel Prize in Chemistry, 1941, for the use of isotopes as tracers in the study of chemical processes
Tl-201 Cardiac Functional Scan
Stros
Rest

PET Fundamentals

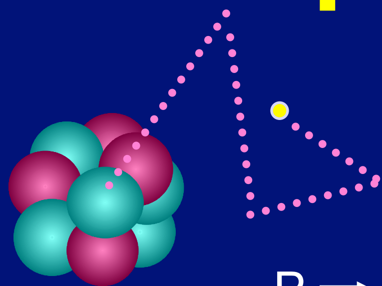

$P \longrightarrow N + e^+ + n + \text{energy}$

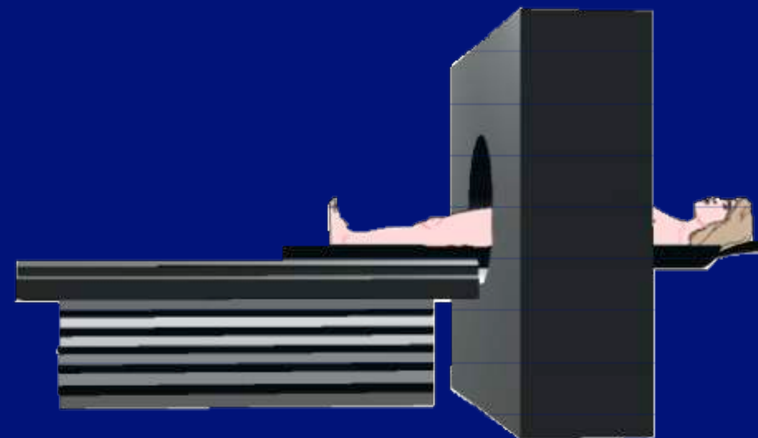

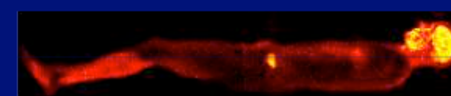

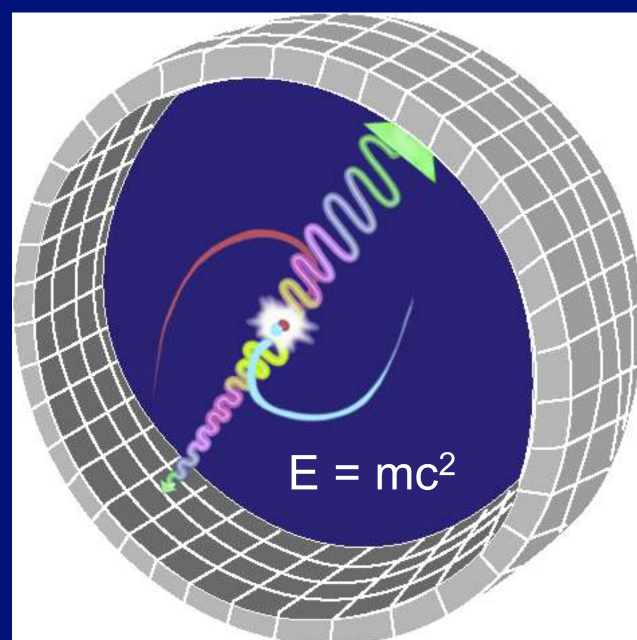

Carl David Anderson (1905-91) received the Nobel Prize in 1936 f or the discovery of the positron.

At age 31, Anderson was then the youngest person to receive the Nobel Prize. (Tsung-Dao Lee got the 1957 prize hen he was 30.)

Production of Isotopes (Cyclotron)

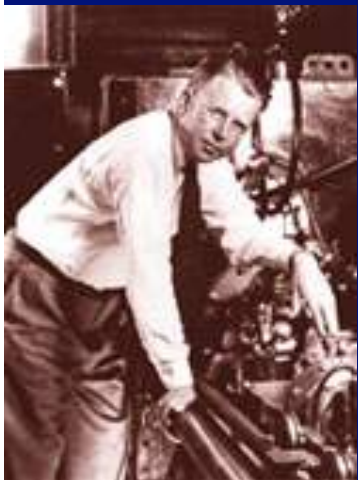

At the ion source of the 184-inch cyclotron in 1948.

The first cyclotron is built in late 1930

Modern Self-Shield Medical Cyclotron

RadioChem Synthesis Module

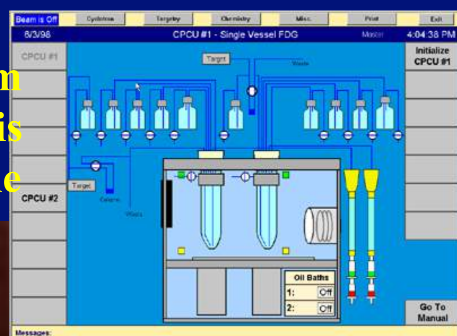

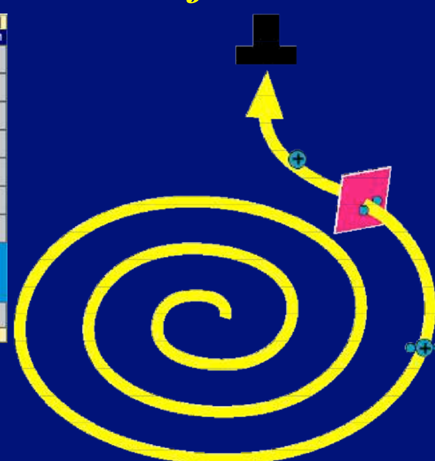

$^{18}O\ (p,n)\ ^{18}F$

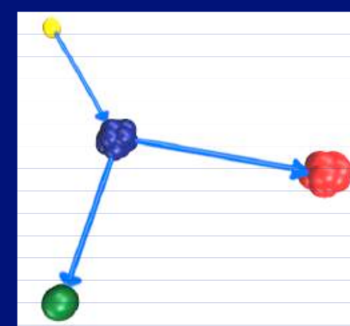

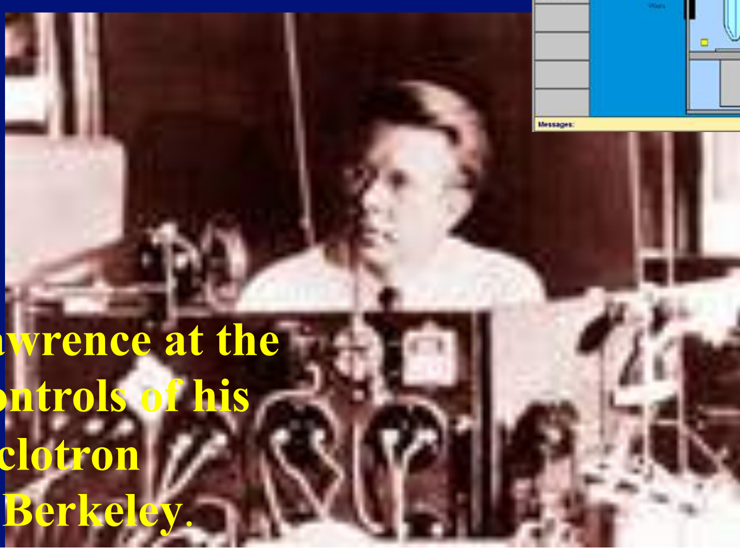

Lawrence at the Controls of his cyclotron in Berkeley.

Ernest Orlando Lawrence (1901-1958) received the 1939 Nobel Prize in physics for the invention and development of the cyclotron

CS-15 Installed at UChicago-ACRH/FMI in 1968

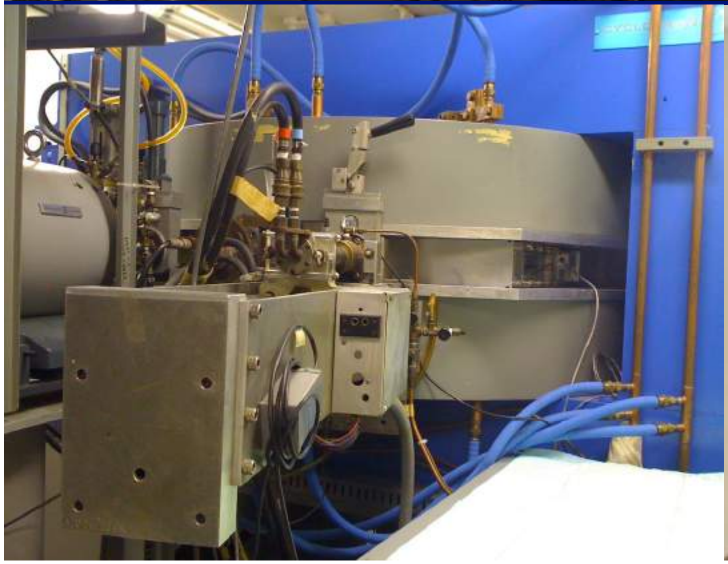

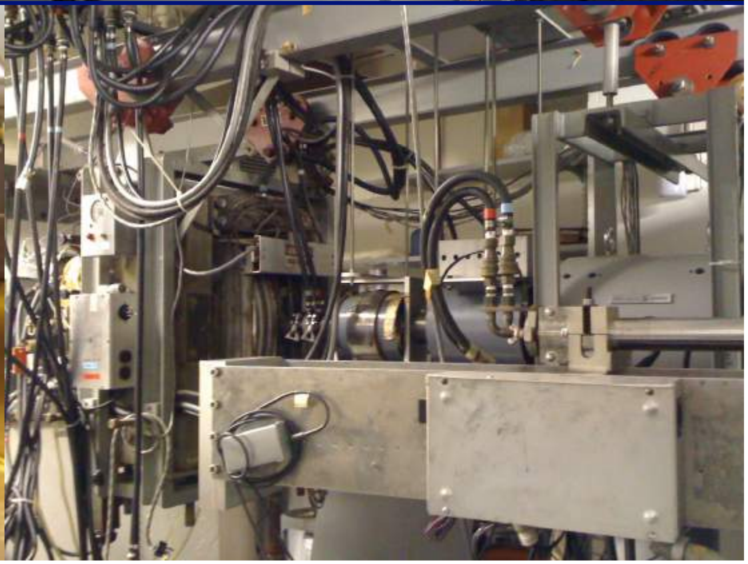

PET Isotopes

^{15}O

^{13}N

^{11}C

^{18}F

^{64}Cu

^{82}Rb

^{124}I

PET Tracers

$[^{15}O]$-O_2 $[^{15}O]$-H_2O

$[^{15}O]$-H_2O $[^{15}O]$-CO

$[^{13}N]$-NH_3 $[^{18}F]$-FDOPA

$[^{13}N]$-glutamate $[^{18}F^{-}]$

$[^{11}C]$-acetate $[^{18}F]$-FDG

$[^{11}C]$-palmitate

[11C]-methionine

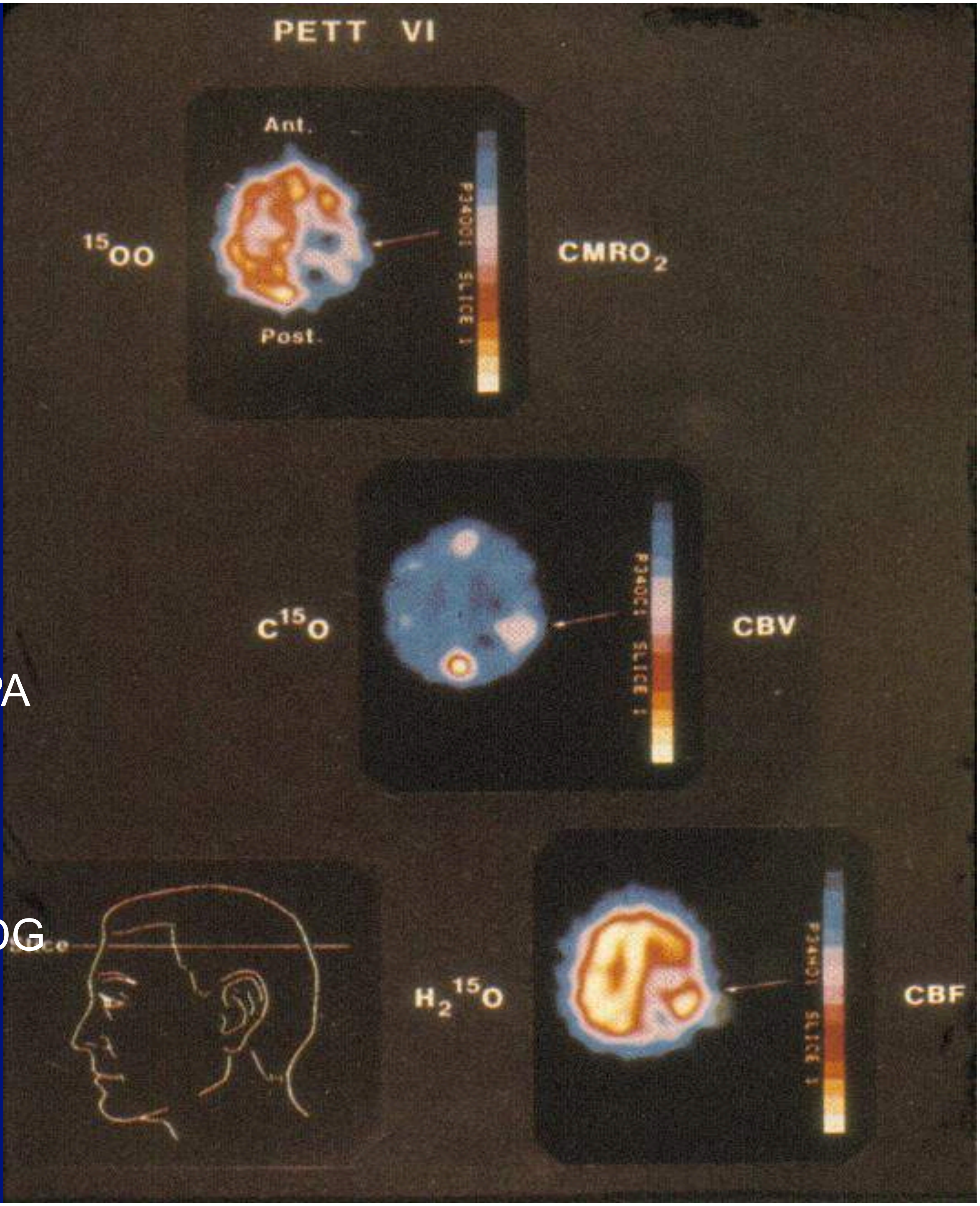

Georges Charpak (1924-2010)

Nobel Prize in Physics, 1992, for his invention and development of particle detectors, in particular the multiwire proportional chamber

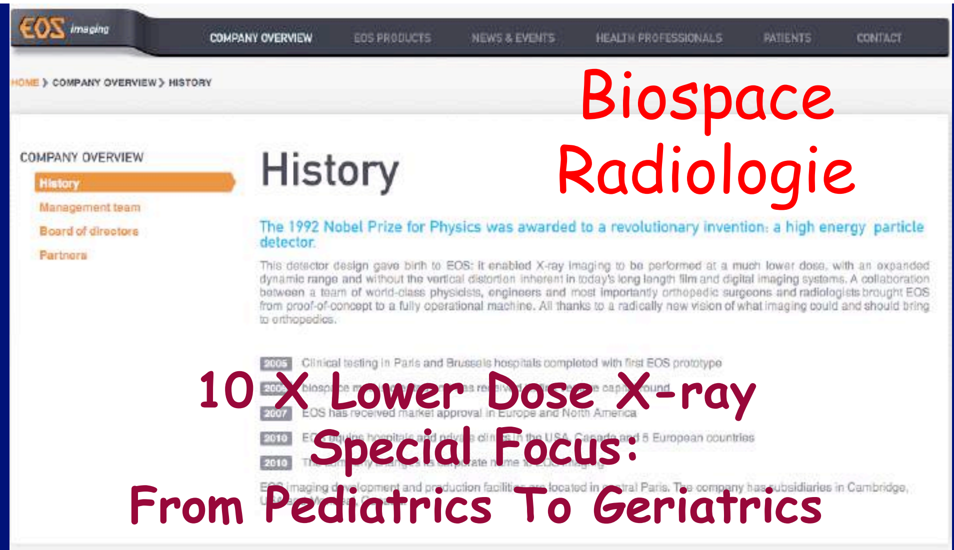

Biospace Radiologie

10 X Lower Dose X-ray
Special Focus:
From Pediatrics To Geriatrics

Fig. 1: EOS 2D/3D System

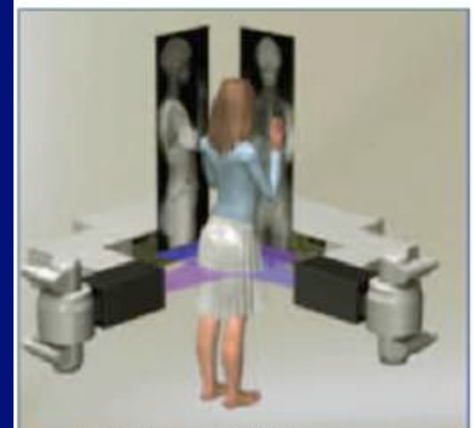

Fig. 2: EOS Scanning Technique
Vertical linear scanning allows the acquisition of long length images without being limited by the detector's vertical dimension. This is particularly important when treating patients whose global balance and posture must be observed.

EOS was developed from ***a Nobel Prize-winning technology*** by a team of engineers, orthopedic surgeons and radiologists as a complete ultra low dose orthopedic imaging solution. EOS allows full-body imaging of patients at a dose reduction up to 90% compared to CR systems

Courtesy of S. Majewski

Magnetic Resonance Imaging (MRI)

Radio Wave, Magnetic Fields

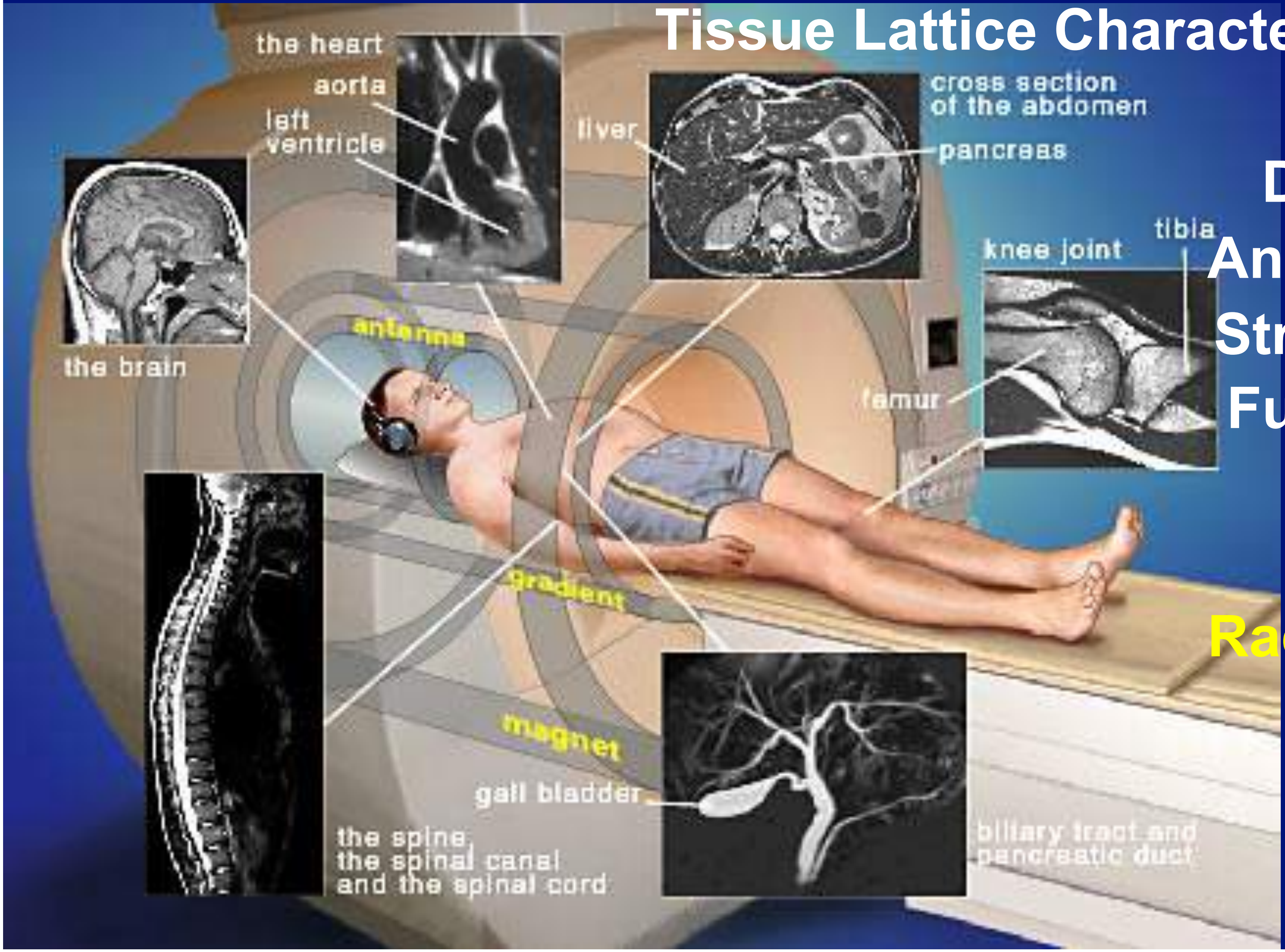

Tissue Lattice Characteristics

Proton

Density

Anatomy/

Structure

Function

3D

No

Radiation

Paul C. Lauterbur (1929-2007) and Peter Mansfield (1933-) received the 2003 Nobel Prize in Physiology or Medicine for their discoveries concerning magnetic resonance imaging (MRI).

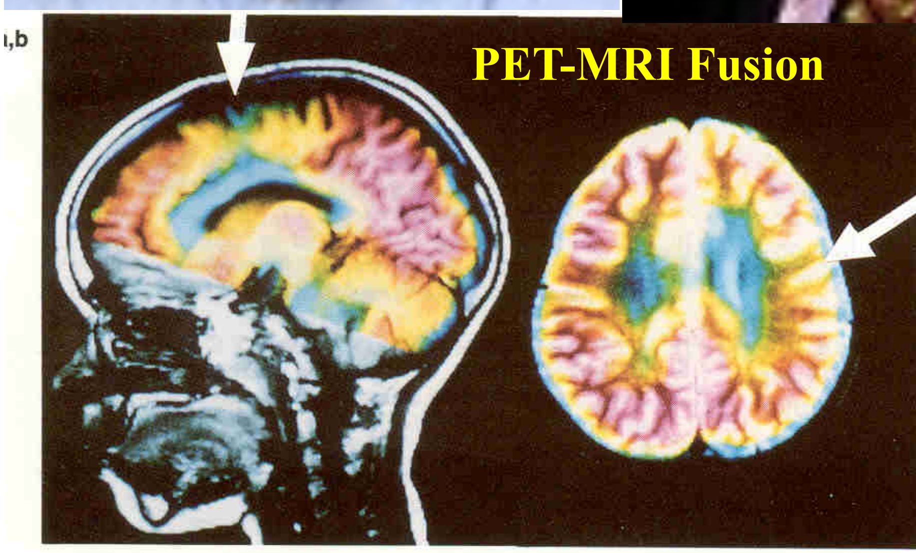

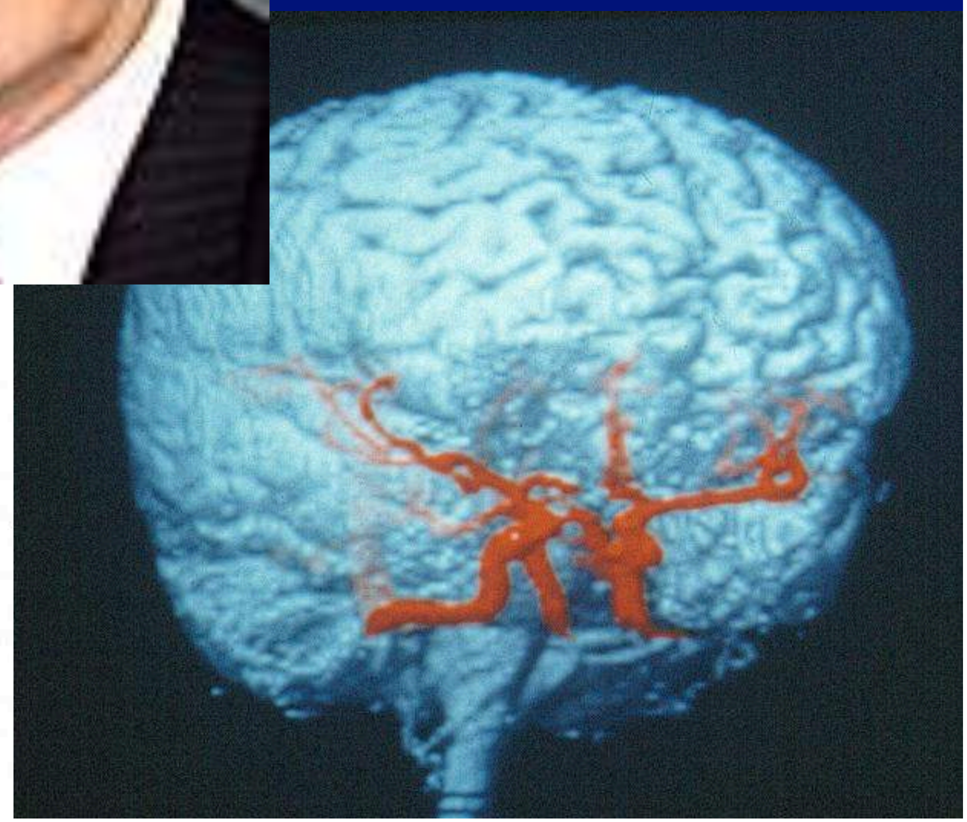

Outlines

- **Mutual Benefits of TIPP & Medical Imaging**

Synergistic Interaction: PP/HEP & MI

1. Common Tech Platforms in PP/HEP & MI
- Radiation Detectors (CsI, BGO, LSO, CdTe, CZT……)
- Photodetectors (PMT, APD, MCP, SiPM……)
- DSP & Fast Electronics (TOF, MTV, TOT……)
- Rapid & Highly-Parallel DAQ with FPGA/CPU/GPU
- Internet/IoT and GRID/Cloud Computing
- Simulation and Data Science (GEANT4, GATE…)

2. Prototyping for Feasibility Validation/Verification
- MI: Small-Scale Prototyping Platform for TIPP
- Technology Assessment, Evaluation, & Validation

CZT/CdTe-Based SPECT Inserts for MRI

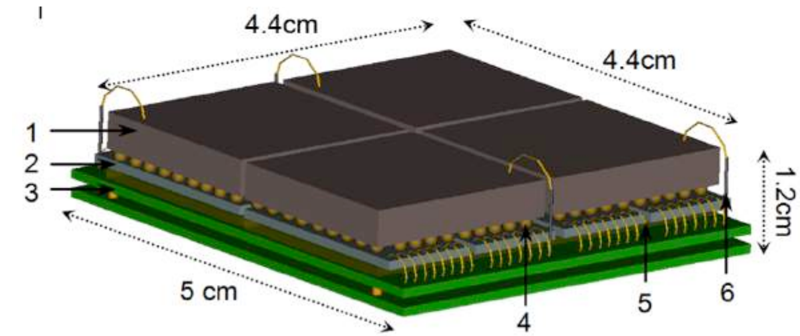

The proposed energy-resolved photon-counting (ERPC) detector. (1) CZT crystals of 4.4cm × 4.5 cm × 2-4 mm in size, (2) ERPC ASICs, (3) Readout PCBs, (4) indium bump-bonding between CZT detector to the ASIC, (5) wire-bonds between the ASIC and the PCBs and (6) Cathode signal out.

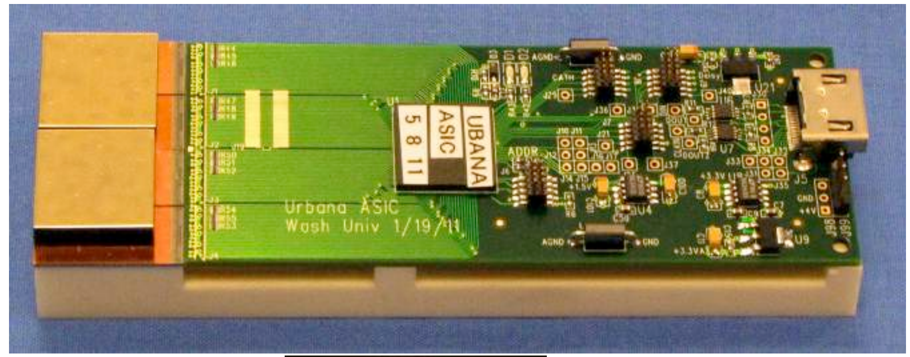

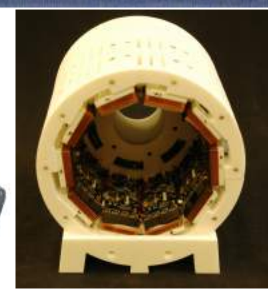

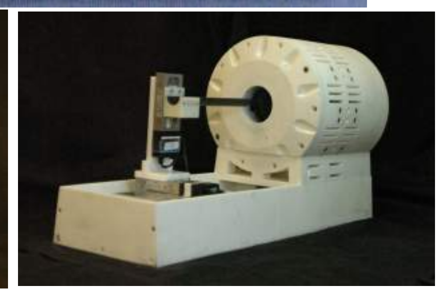

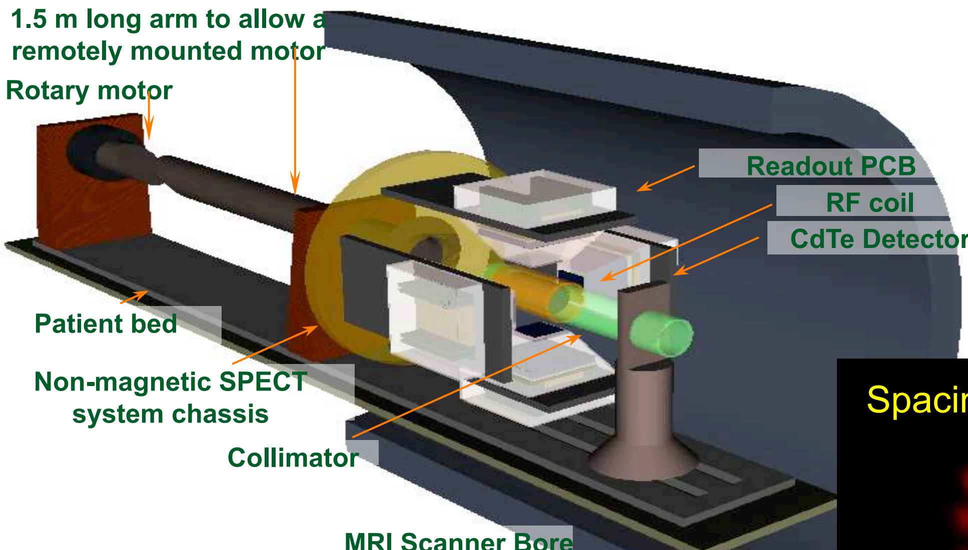

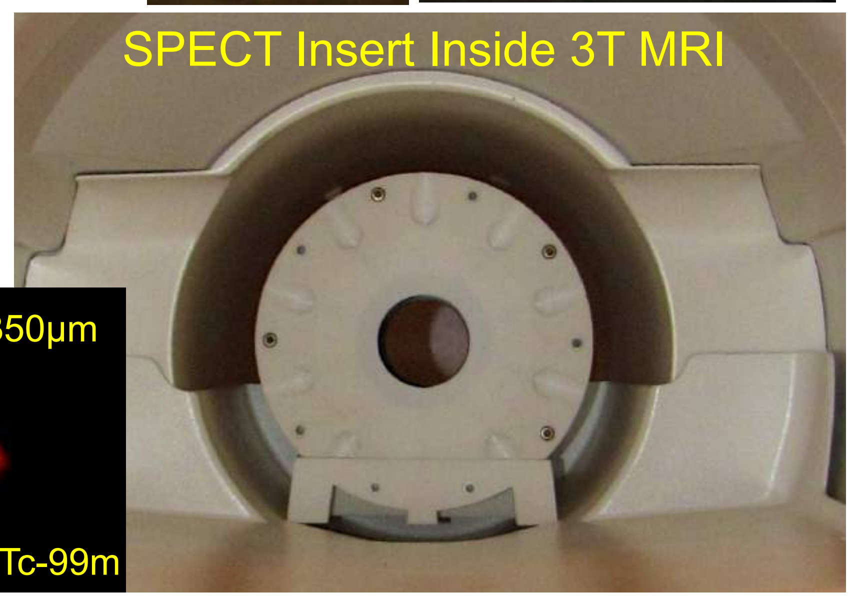

Cai et al, NIMA, 2014
UIUC-Meng et al & UC-Chen et al

SPECT/MRI Brain Imaging in 3T & 14.1T MRI

Lesniak/Balyasnikova (NWU); Meng (UIUC); Chen (UChicago)

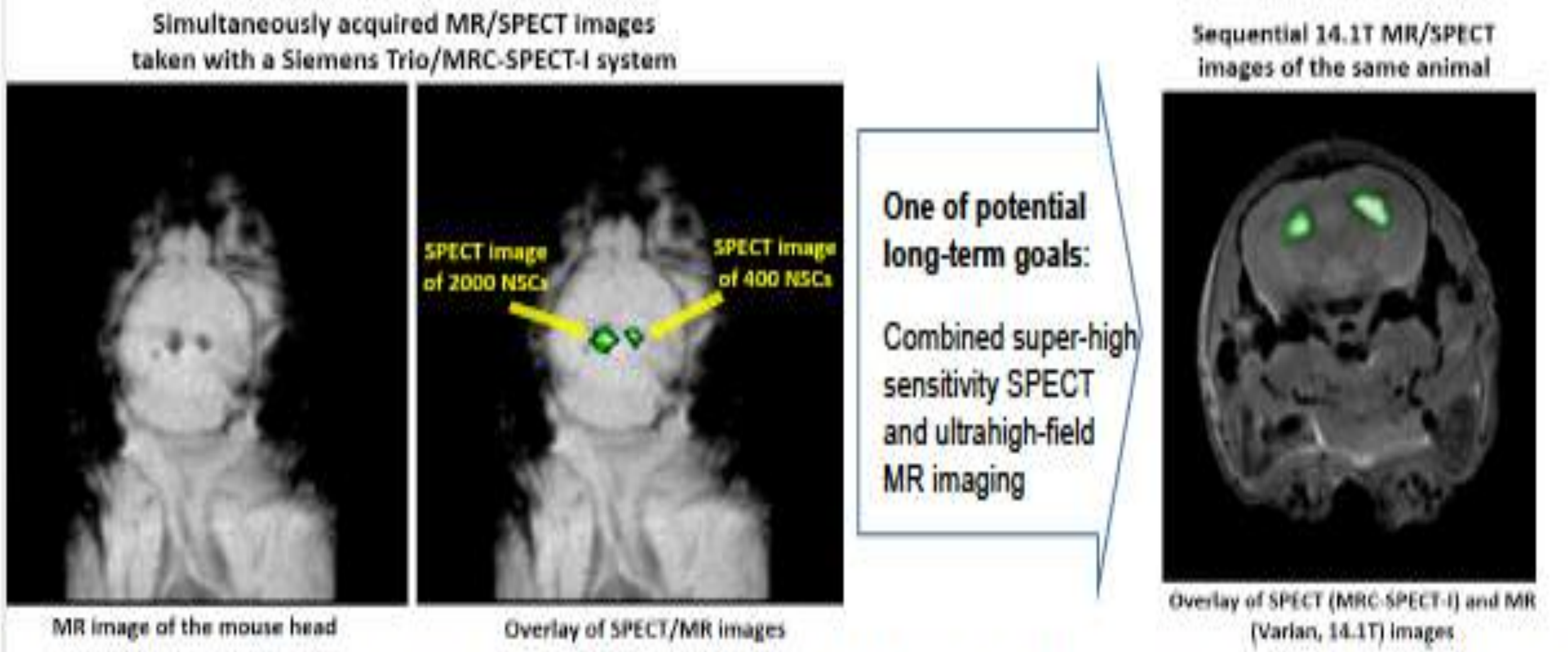

Fig. 5: SPECT/MR images of NSCs taken with the UIUC MRC-SPECT-I system with a Siemens Trio clinical scanners (**left and middle**) and an ultrahigh field (14.1T) Varian MR spectrometer (**right**). The 3T MR image was acquired with gradient-echo, voxel size: 0.3 mmx0.3 mm x1.5mm, sample bandwidth 230HZ, T_R 300ms; T_E 5.00ms, flip angle 25, imaging time: 9mins38s. The SPECT image of the stem cells (labeled with In-111 Oxine) was acquired with 1-hour, and the images were reconstructed using MLEM algorithm.

CdTe/CZT For Next-Generation Spectral (Color) CT

Iwanczyk (DxRay) et al, IEEE TNS 2009

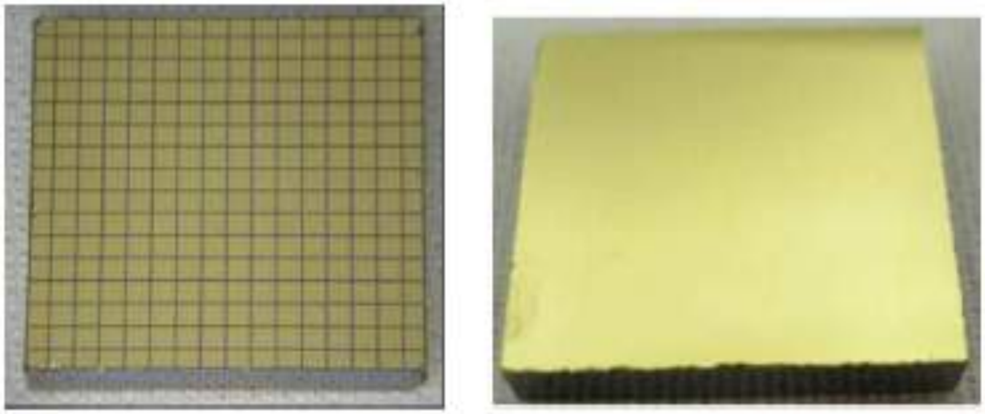

Fig. 1. A photograph a CdTe crystal with a 16 × 16 pixel anode structure at a pixel pitch of ~ 1 mm on one side (shown on left) and a continuous cathode on the other side (shown on right).

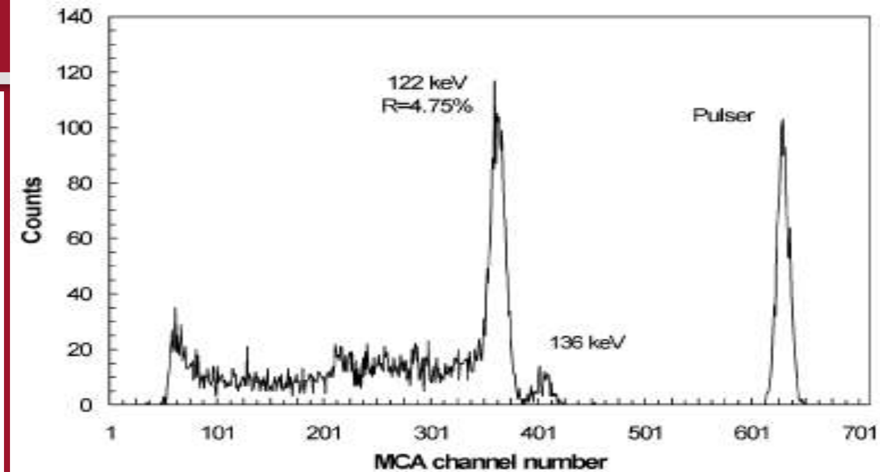

Fig. 3. Spectrum taken with a single detector pixel in response to Co-57 source using a short shaping time. Electronic noise is represented by pulses injected from an external generator (pulser peak).

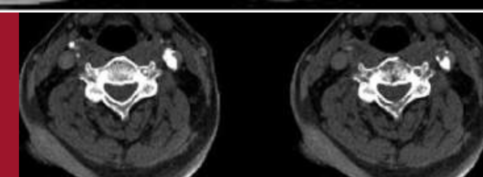

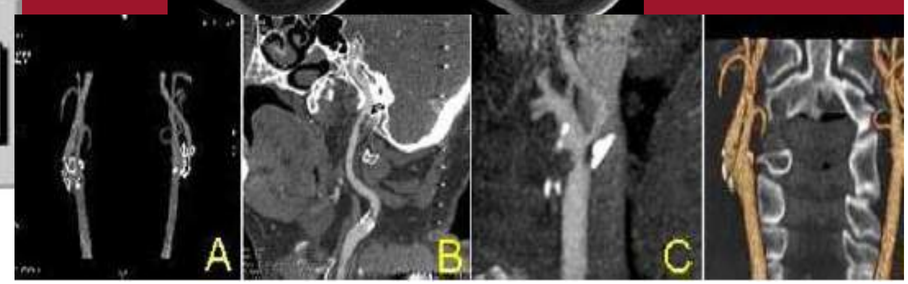

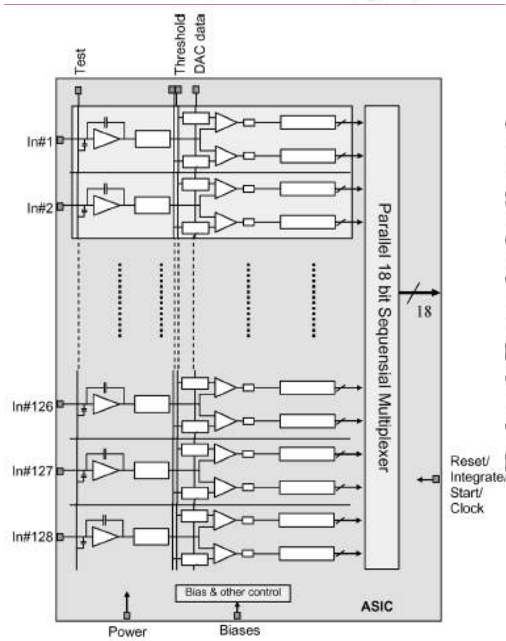

Fig. 7. The full ASIC architecture.

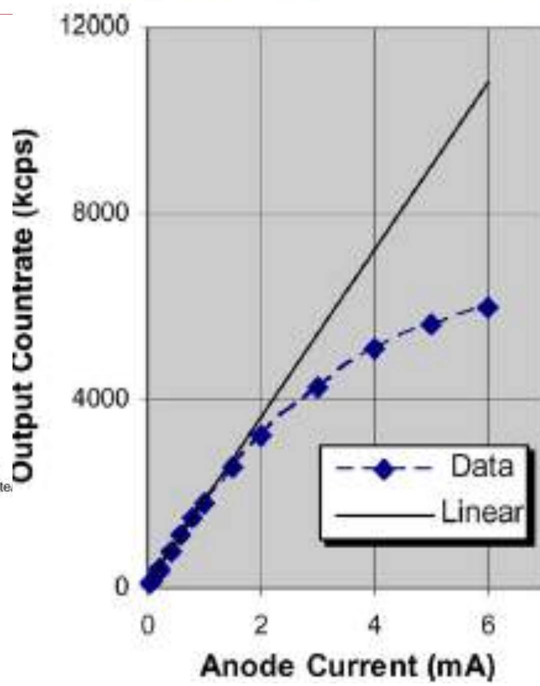

8” X 8” MCP Development from LAPPD for TOE-PET

Kao/Kim/Chen (Medical Physics) & Frisch (HEP) + ANL/FNAL

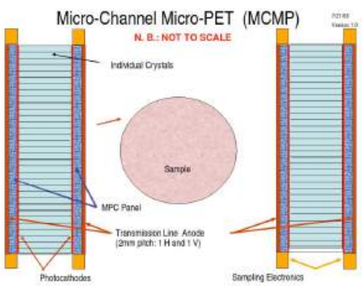

- Two detector modules facing each other.
- One detector module consists of 24x24 array of LSO scintillator and 2 MCP/TL assemblies.
- LSO pixel dimension : 4x4x25mm^3.
  - Crystal pitch : 4.25mm
- MCP assembly dimension : 102x102x9.15mm^3. (4”x4” of area) photocathode and TL structure are included.
- MCP/TLs are coupled to LSO at both front and back ends.
- Waveform sampling (20GSPS) for DAQ.

24”x16” Super-Module (Mock-up)

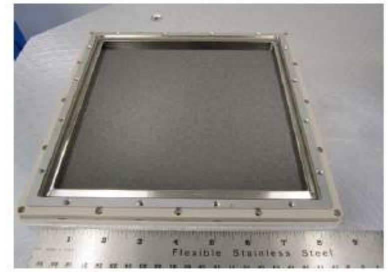

8”x8” MCP (Ossy Siegmund, SPIE2011)

The study shows the design is suitable for TOF PET.

~11% FWHM of energy resolution at 511 KeV.
~320 ps FWHM coincidence time resolution.
~2.5 mm FWHM for position accuracy along a TL.
DOI Correlation in energy and time measured forward/back MCP/TL.
Cf. ‘A design of PET detector using MCP PMT…’, NIMA 622 (2010) p.628

Large Area Picosecond Photo-Detector (LAPPD) project

- Aiming to develop large area (8”x8”) MCP-PMT
- Collaboration of Univ. of Chicago, Argonne, Fermilab,….
- Estimates a factor of ~10 cheaper than PMT per area.

When available, it can be applicable to PET instrument.

- Various PET design would be possible at reasonable cost.

For more info on LAPPD project, http://psec.uchicago.edu/

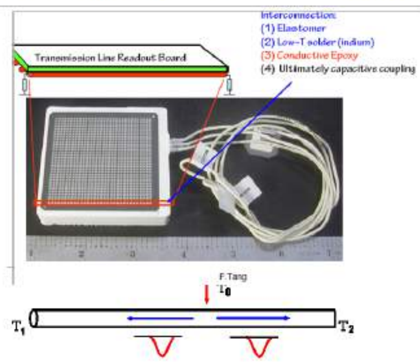

- Two correlated signals propagate to both ends.
  - Timing : (T1+T2)/
  - Position along TL : (T1-T2)
  - Energy : Q1 + Q2
- An efficient way for large area readout.
  Scales to L, not L^2 as the area(L x L) increases.
- Require precise time decision.
  Waveform sampling.

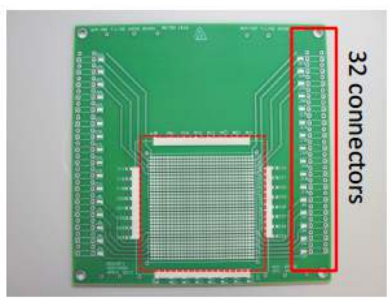

Transmission-line board

- **Prototype Transmissioin-Line board**
- 32 micro-strip Z=50Ω lines
  Width = 1.1mm, Pitch = 1.6mm
- Matches anode structure of XP85022
- Solder the MCP anode on the board.
- need (32+32) readout channels.
  (32 + termination with 50Ω).

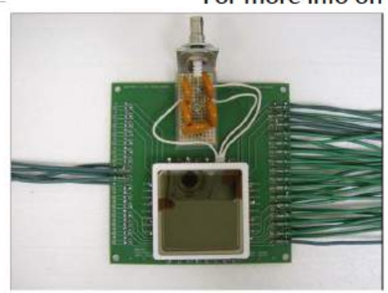

Prototype MCP PMT/TL module.

3 units were built.
(32 + 4) channels are connected.

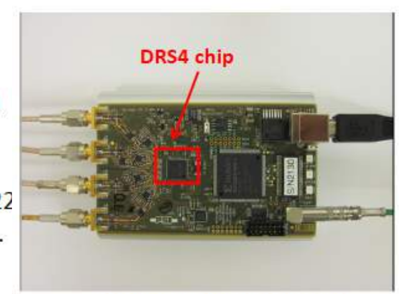

DRS4 evaluation board

Domino Ring Sampler (DRS)

Switched Capacitor Array (SCA) technology.
Developed at PSI, Switzerland.
Sampling : 700 MSPS – 5GSPS
8+1 channels in one chip.
1024 sampling capacitors in one channel.
200 ns sampling range at 5GPS.
1 V of input dynamic range.
Need external ADC for digitization.
Analog bandwidth : 950MHz (-3dB)
Low power consumption : 10-40mW / channel

DRS4 evaluation board (available from PSI)
4 input channels.
USB 2.0 interface for DAQ.

SiPM – Enabling Novel PET System Designs

GE Signa PET/MRI
Hammamatsu SiPM
LBS Crystals
TOF < 400ps
25 cm Axial FOV
4.4 mm FWNM @ 1cm
21kcps/MBq Sensitivity

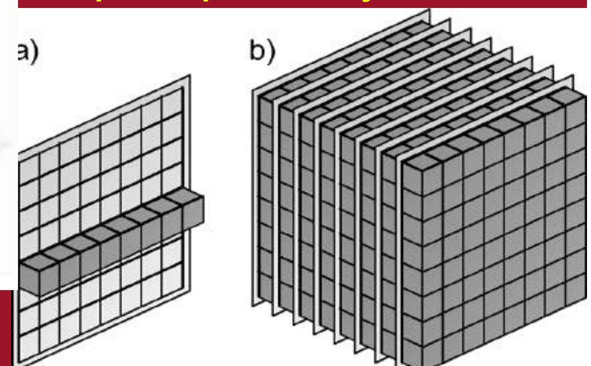

Other Innovative Designs
Sandwiched, double-sided
Side-lined, etc. for DOI
and other information

Philips Vereo PETCT
PDPC dSiPM
LYSO Crystals
TOF 325ps
16-25 cm Axial FOV

Parameter	Gemini TF16	Vereos
LYSO detectors	28,336	23,040
Resolution	4.8 mm	4.1 mm
Sensitivity*	6.6 kcps/MBq	22.0 kcps/MBq
Peak NECR*	125 kcps	650 kcps
	@ 17 kBq/ml	@ 50 kBq/ml
Timing	585 ps	325 ps
Axial FOV	18.0 cm	16.4 cm

Strip-Line (SL) and Waveform Sampling (WS) DAQ

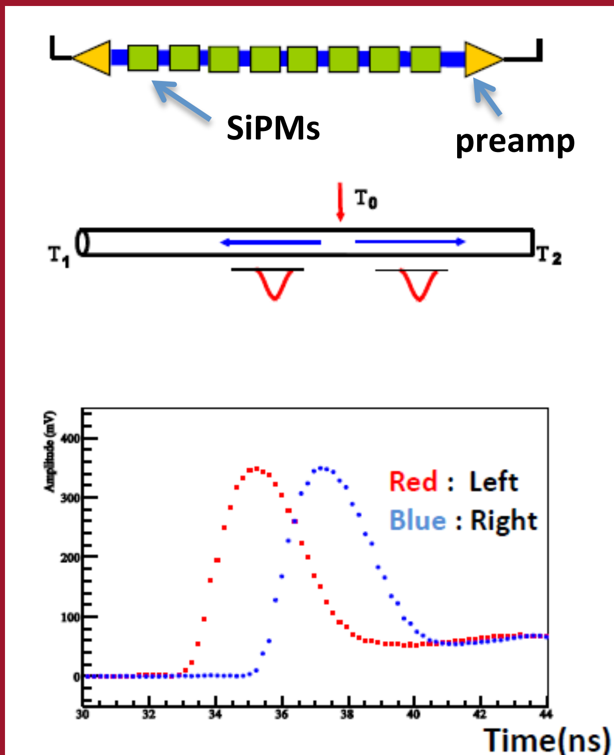

Waveform sampled at the two ends.

The position of the firing SiPM (or other PD) is determined using the propagation time difference.

PET signal pulse

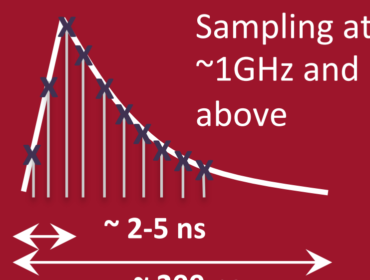

Domino Ring Sampler

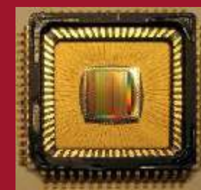

DRS4 chip, 0.8-5 GHz sampling, 8 channels

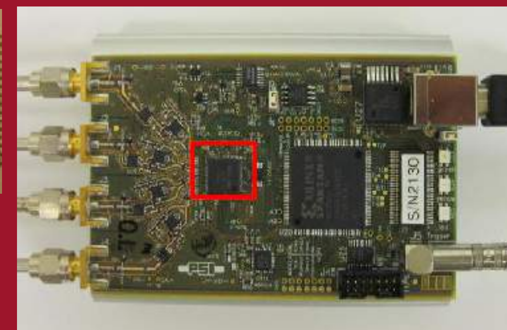

DRS4 evaluation board (4 ch)

Switched capacitor array (analog memory)

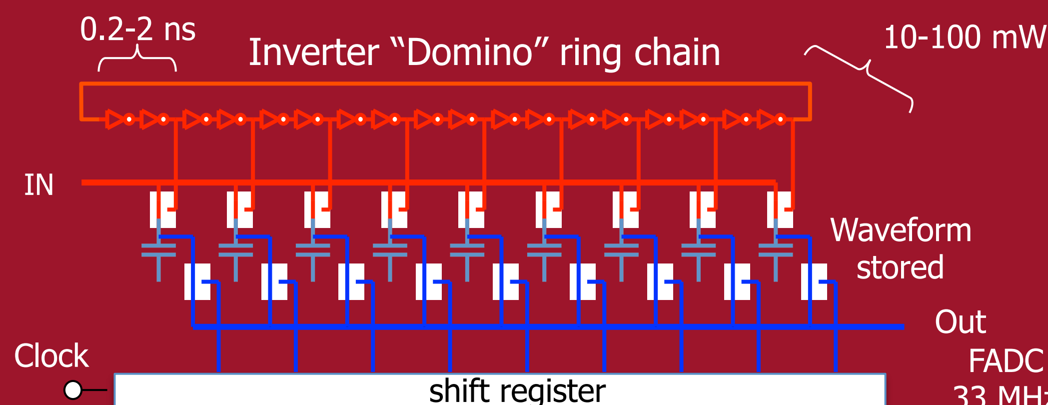

SL-WS DAQ - PET Insert for 4.7/9.4/14.1T MRI

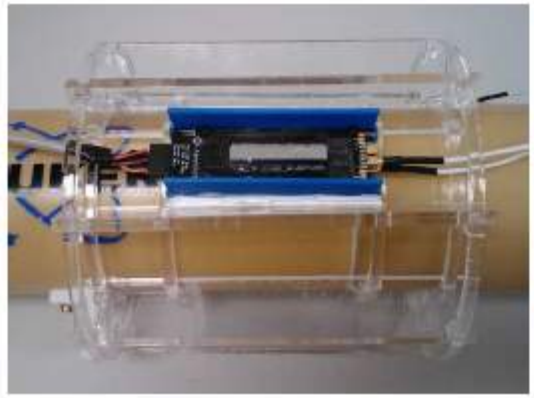

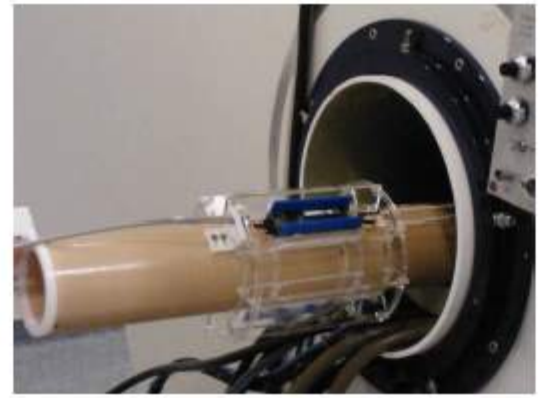

8x2 LYSO crystals/SiPMs read by using 2 strip lines

A prototype MRI insert holding 8 modules

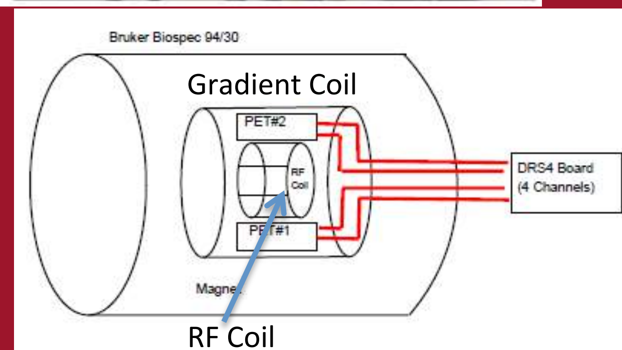

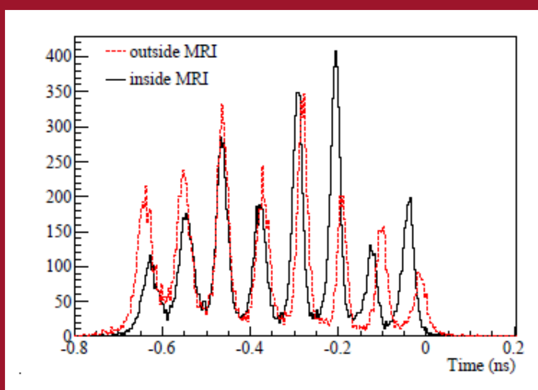

Identification of crystals (5.2mm pitch)

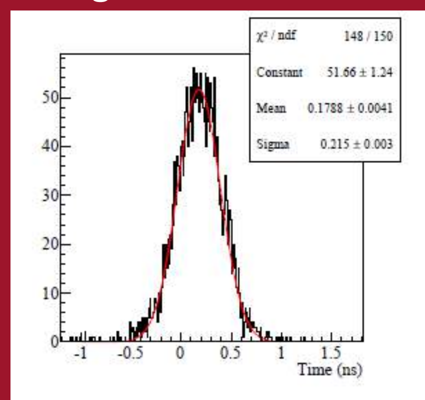

Coincidence timing resolution ~500 ps FWHM, in/out MR

Insert in a 9.4T Bruker scanner, main DAQ electronics are outside in the control room

Kim et al, 2015, NIMA

Multi-Voltage Threshold (MVT) Sampling DAQ

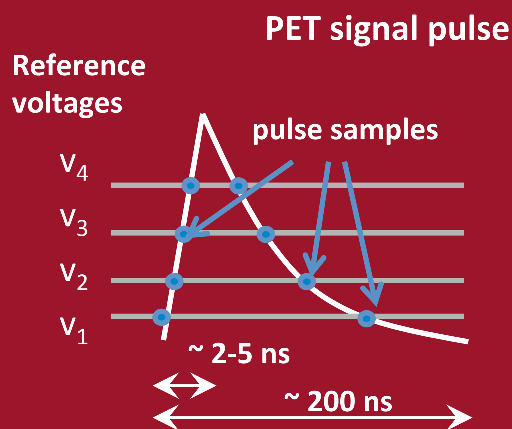

Proof of principle (by simulation: Xie et al, TNS 2005, by measurement: Kim et al, 2009)

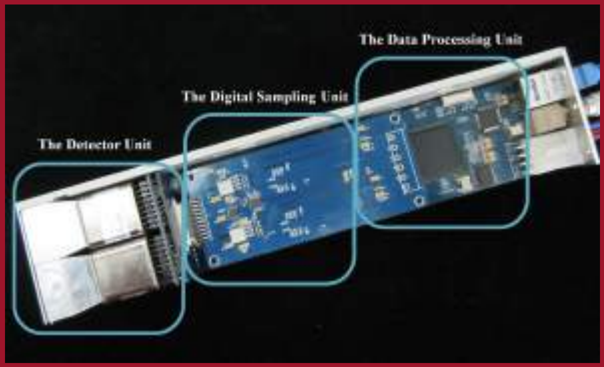

Implementation (Xie et al, TNS 2012)

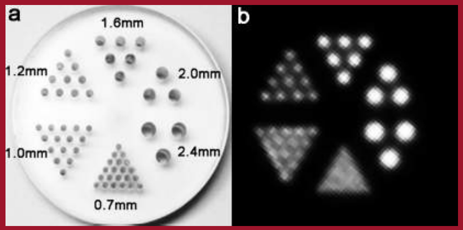

The Trans-PET BioCaliburn LH
FOV: 13 cm ϕ, 5.3 cm length
Commercial system (Wang et al, PMB 2014, pending minor revision)

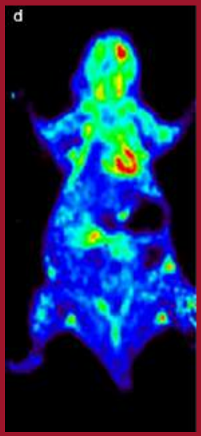

35g mouse/FDG

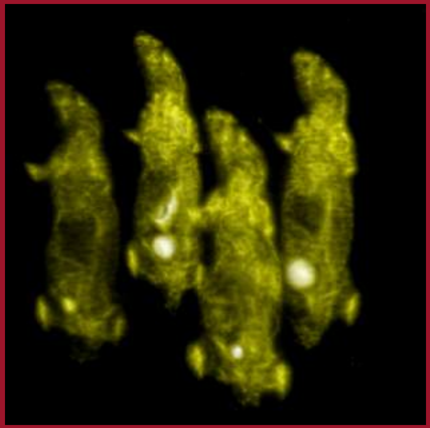

Simultaneous imaging of four mice

Initial Simulation Results - GATE

Whole-body phantom

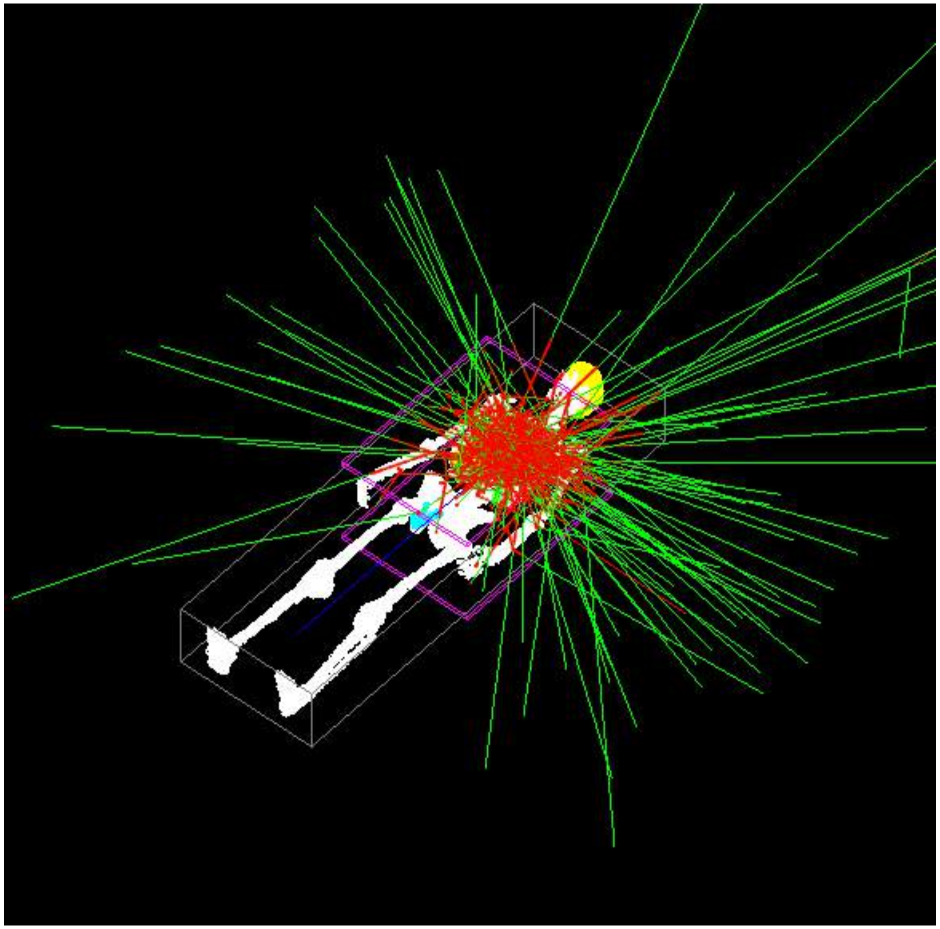

Have obtained a 6-minute scan (1-minute frame)

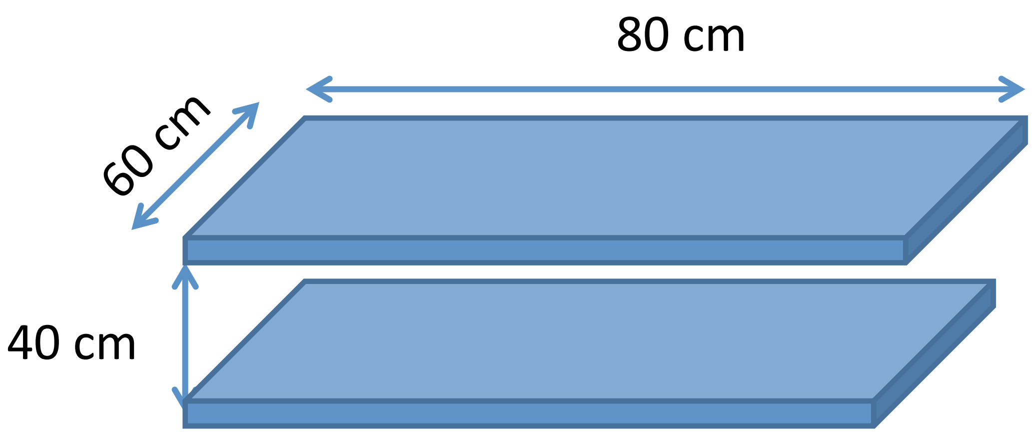

LAPPD PET

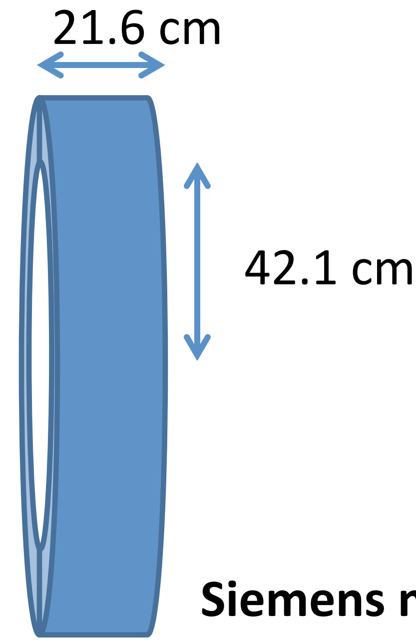

Siemens mCT

- Two 80x60 cm^2 LAPPD detectors, 4x4x20 mm LSO crystals, 40 cm spacing; axial FOV =80 cm
- energy res. 15%; perfect time resolution
- Count statistics (simulation):
  - Zubal phantom (~191 lbs); **2mCi** injected; scan starts right away
  - 450-650 keV energy window, 3.5 ns time window, 210-second scan
  - 54M trues+scatters, 9.9M randoms; scatter fraction ~32%, random fraction~21.28%

- 84.2 cm-diameter detector ring, 4x4x20 LSO crystals, 52 rings; axial FOV = 21.6 cm (33% longer than others); 4 bed positions to cover ~80 cm
- energy res. <12%; time res ~ 555ps
- Count statistics (measurement reported):
  - 160 lb patient; 16 mCi injected; scan starts 90 min post injection (~**9.1 mCi** at start of scan)
  - 350-650 keV energy window, 4.5 ns coincidence window; 210-second scan
  - 44M trues+scatters, and 67M randoms; scatter fraction ~30%, random fraction ~68%

Comparison – Regular & Long Axial FOV Scanners

- 2mCi with LAPPD PET vs. 9.1mCi with mCT:
  - LAPPD PET has more trues+scatters (54M vs 44M, 10M or ~23% more)
  - LPPPD PET has much fewer randoms (9.9M vs 67M due to use of lower dose)
  - For NECR=T^2/(T+S+R) (a measure of SNR-equivalent count): LAPPD is ~21.0M and mCT is only ~8.54M, ~2.5x gain.
  - LAPPD PET uses 22% dose but yields 23% more trues (and scatters) and a SNR gain of ~2.5. This does not consider the effect of TOF measurement.
  - TOF: 555 ps with mCT => an additional SNR gain of 1.36, 1.67, or 2.36 due to TOF if the LAPPD PET system has a TOF resolution of 300 ps, 200 ps, or 100 ps.
  - An order of magnitude reduction in dose is possible.

Outlines

- **Forward-Looking Applications: Challenges & Opportunities**

NCI Provocative Questions Initiatives

2011- PQ - 13

Can tumors be detected when they **are** **two to three orders of magnitude** ***smaller than those currently detected with in vivo imaging modalities?*** Background: Current imaging modalities allow detection of tumors composed of ***approximately 10^7 cells or in the range of 1 cubic millimeter***. Any increase in imaging sensitivity provides valuable ……

Targeting Novel Imaging Tracers X ~ 5-20

Targeting Novel Imaging Tracers X ~ 5-20

Innovative Image Reconstruction, Processing, Analysis, & Computing X ~ 5-20

BLI & SPECT/CT Tracking of Brain Tumor

Lesniak et al (NWU)
Meng et al (UIUC)
Chen et cl (UChicago)

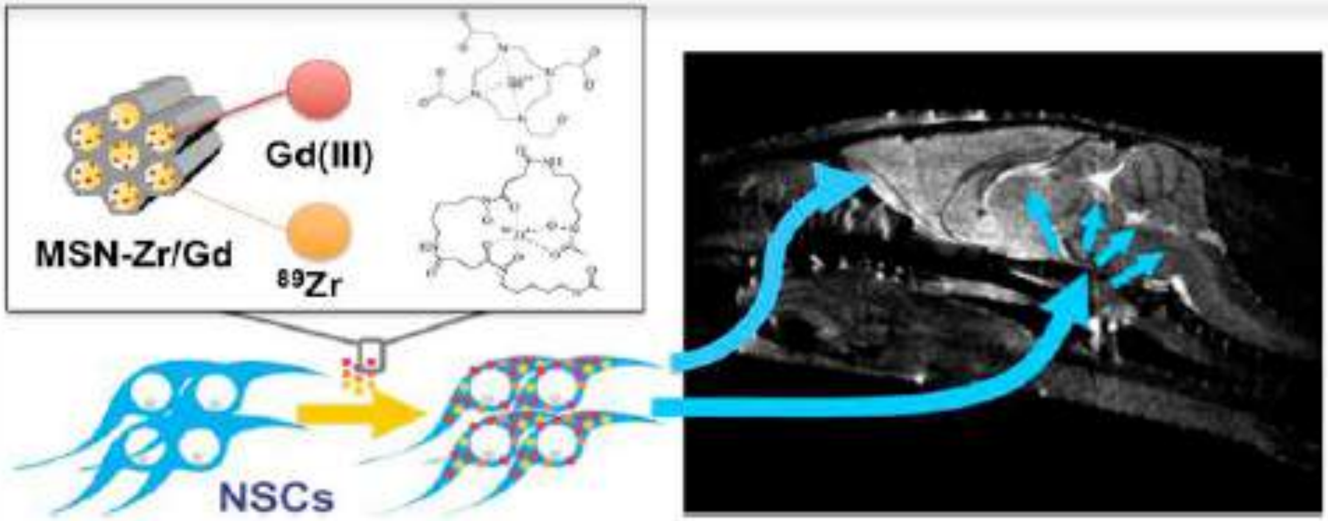

Carrier - **Mesoporous Silica Nanoparticle (MSN)**

Targeting & Thera-peutics - **Neural Stem Cell (NSC)**

Imaging Probes – **Gd/In-111/Zr-89**

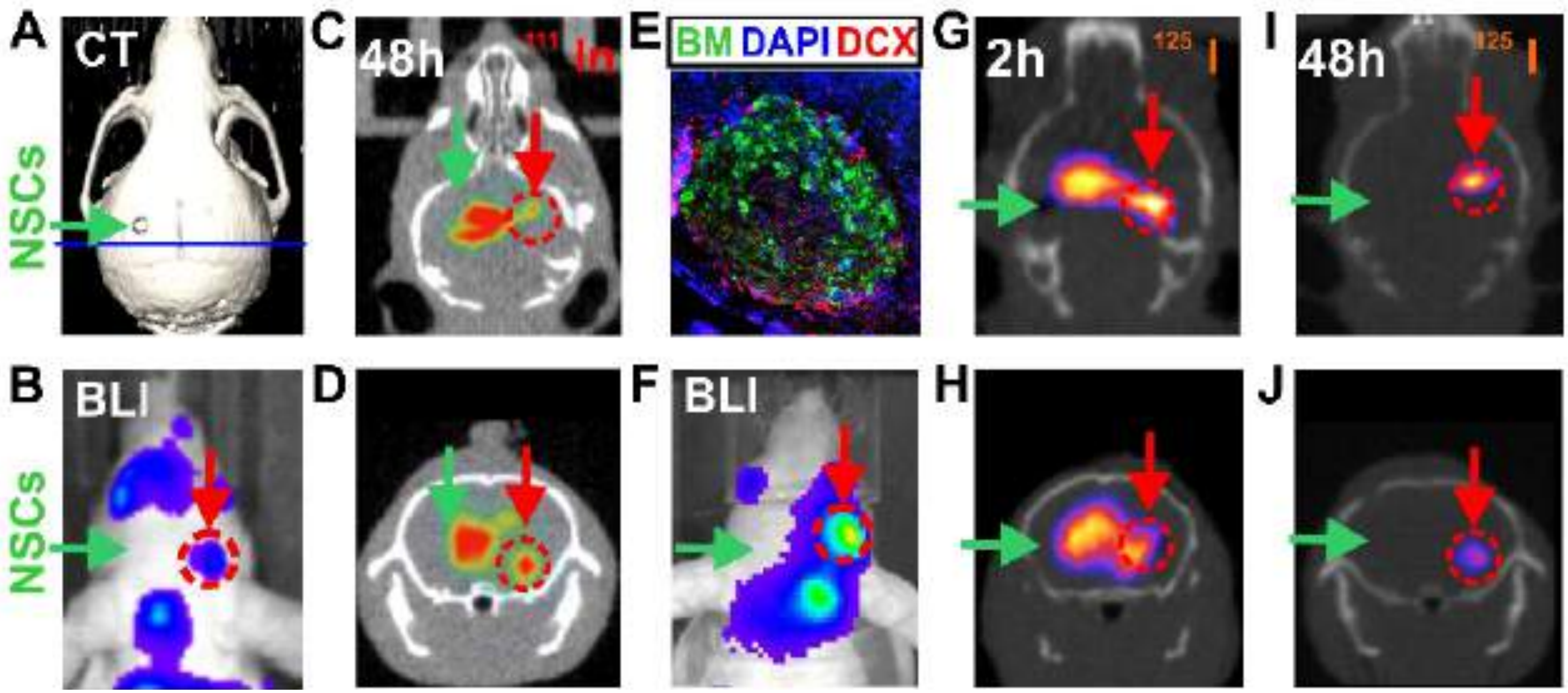

Dynamic In Vivo SPECT Imaging of Neural Stem Cells Functionalized with Radiolabeled Nanoparticles for Tracking of Glioblastoma

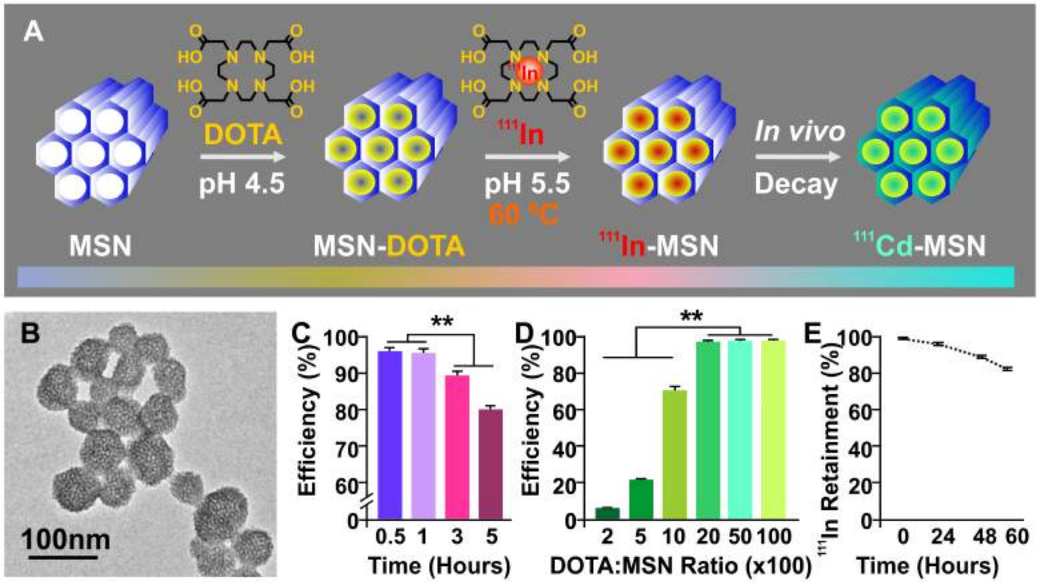

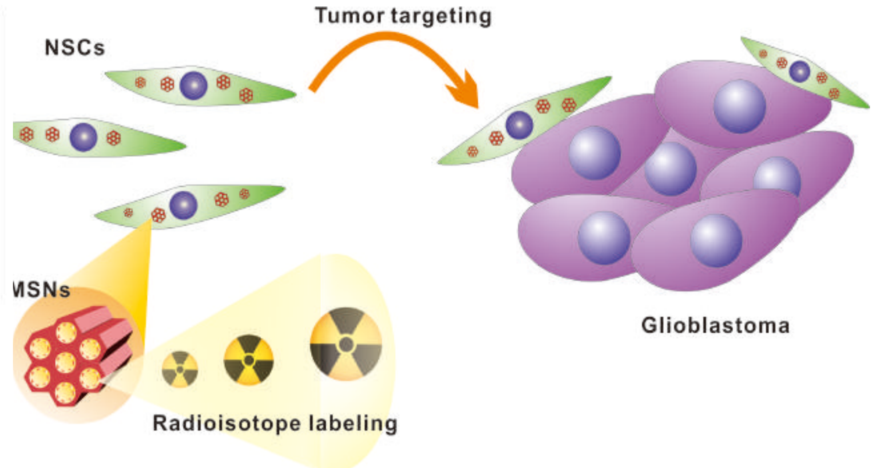

RadioNanoTheranostics

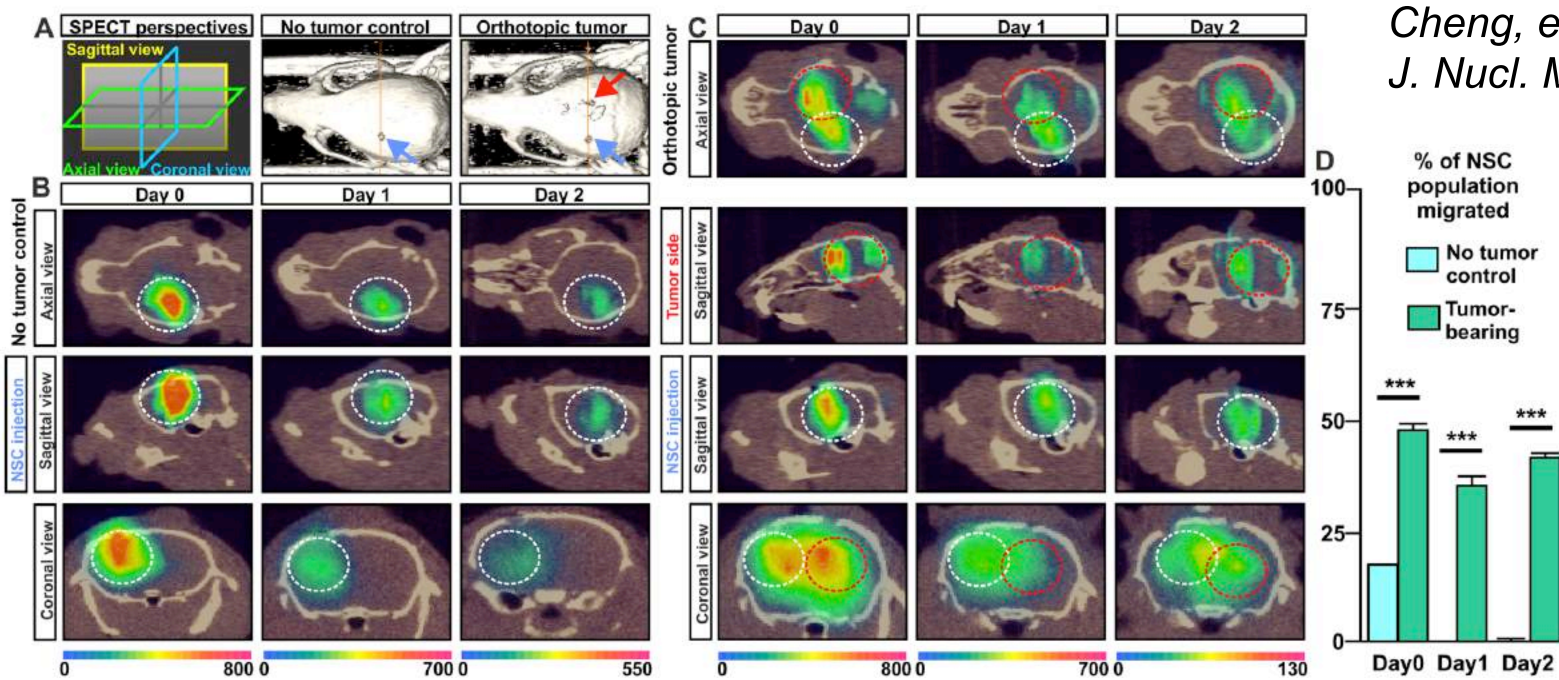

Cheng, et al
J. Nucl. Med. 2016

Inverted Compound Eye (ICE) SPECT

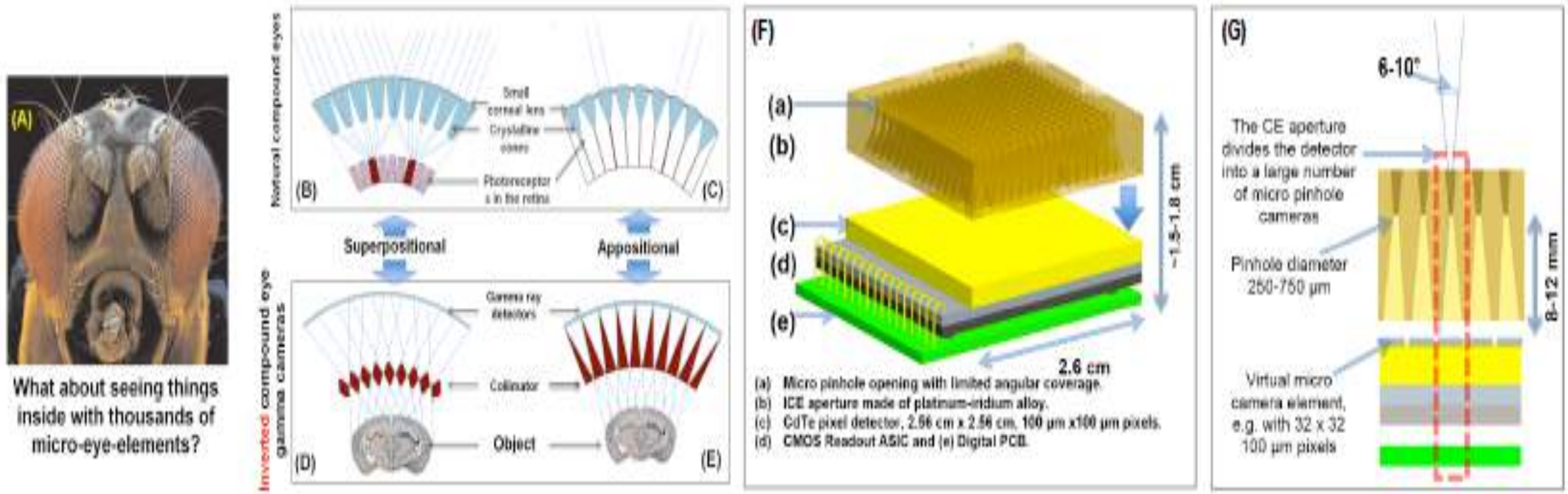

Fig. 2: Natural apposition compound eye and the proposed inverted compound eye camera concept. (A) Head of the fruit fly 'Drosophila melanogaster'. (B) Refracting superposition compound eye. A large number of corneal facets and bullet-shaped crystalline cones collect and focus light – across the clear zone of the eye – towards single photoreceptors in the retina. (C) Focal apposition compound eye. Light reaches the photoreceptors exclusively from the small corneal lens located directly above. This eye design is typical of day-active insects. (D) Schematic of a superposition inverted compound eye camera based on an ultrahigh resolution gamma ray imaging detector. (E) Appositional inverted compound eye camera. (F) Tentative design of the Inverted Compound Eye (ICE) camera module. (G) Cross sectional view of the micro pinhole-camera elements.

Sensitivity:~8X10^{-4} cells/ml → A Factor of 8 To Go

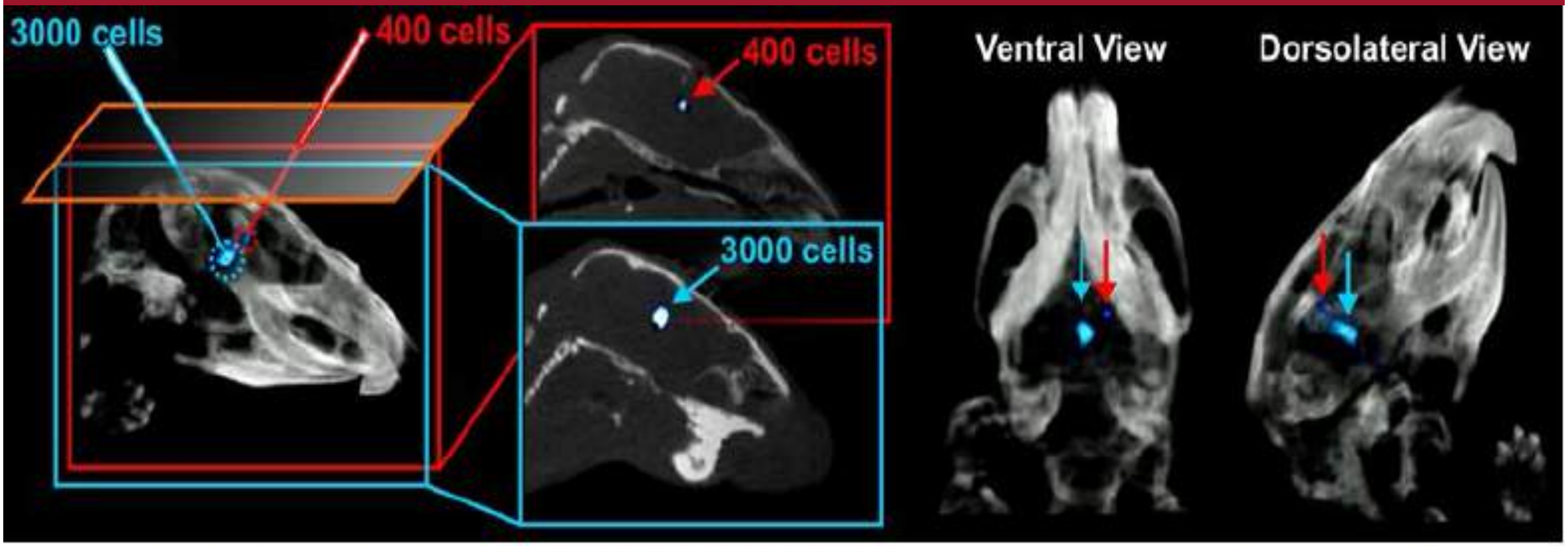

Fig. 4: 3-D rendering of a fused SPEM/CT image of the mouse's head. Two groups of In^{111} labeled NSCs (5 μL and 14 μL in volume as shown with red and blue arrows respectively) were injected into the left and right striatum. The total imaging time was 2h. Images were reconstructed using the data sets corresponding to 400 and 3000 cells. Sagittal, ventral and dorsolateral views are shown.

PET/CT Tracking

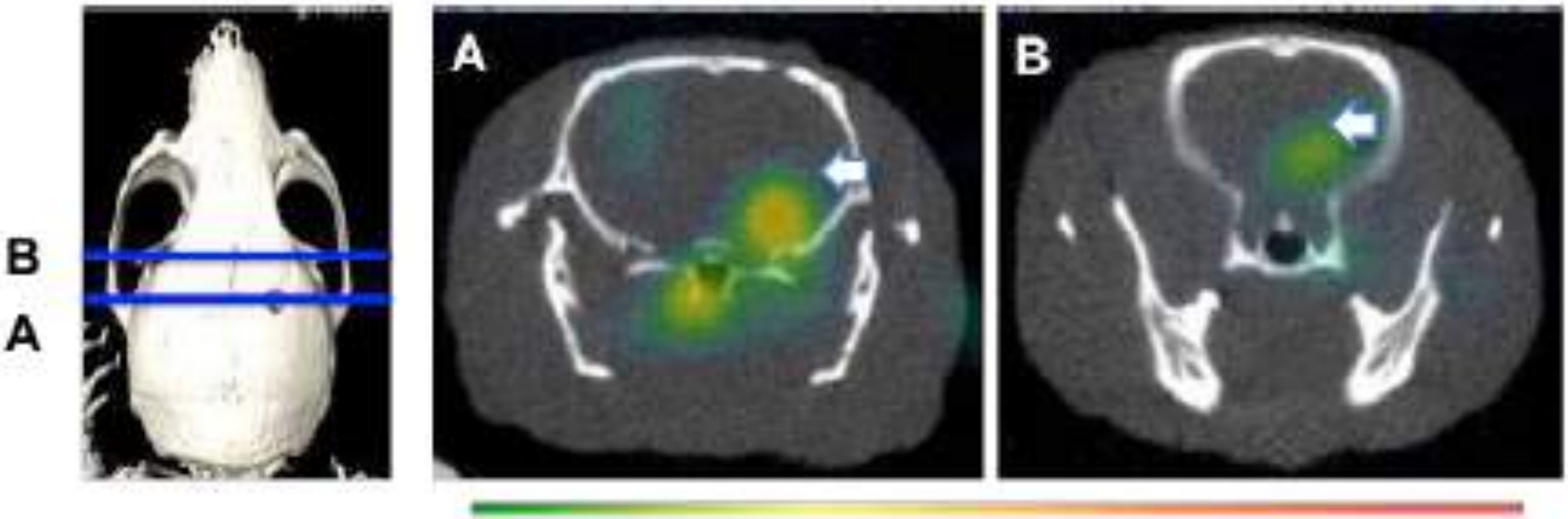

Figure 3: The PET image (coronal view) of ^{89}Zr-MSN-loaded NSCs migration to GBM animal xenograft (A) 24 hr (B) 48 hr post IN administration. White arrows indicate GBM.

EXPLORER: Total-Body PET

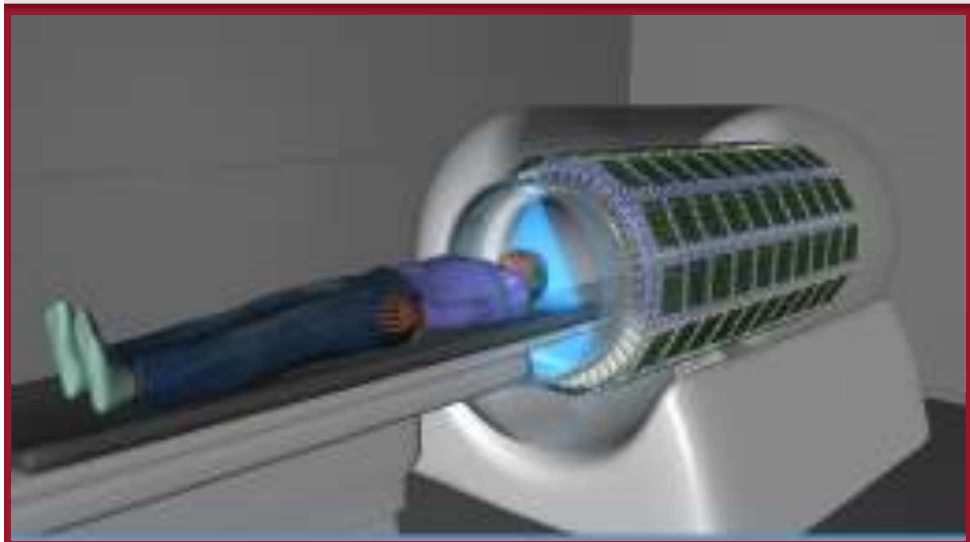

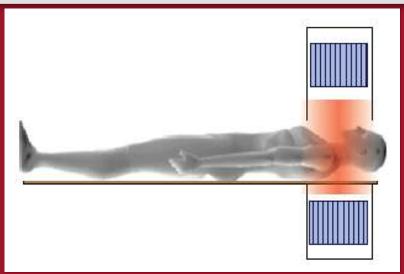

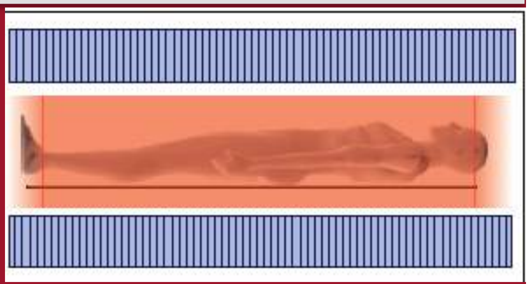

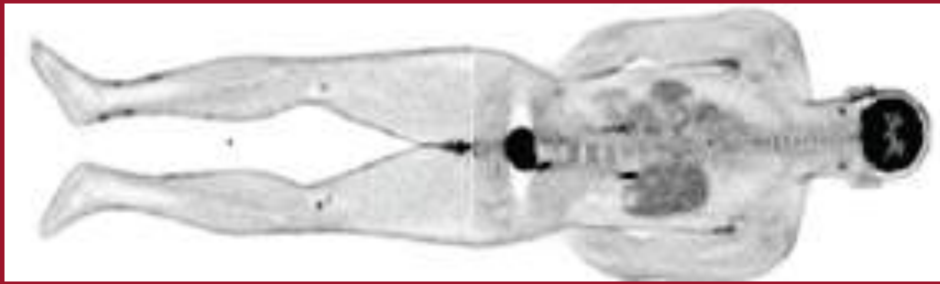

- x40 gain NEC!
- Higher statistics
  - Support higher spatial resolution
- Lower radiation dose
  - Whole body scans at ~ 100 μSv
- Higher dynamic range
  - Late imaging, 5 more $T_{1/2}$
- Whole-body kinetics
  - Better temporal resolution
  - All tissues/organs simultaneously

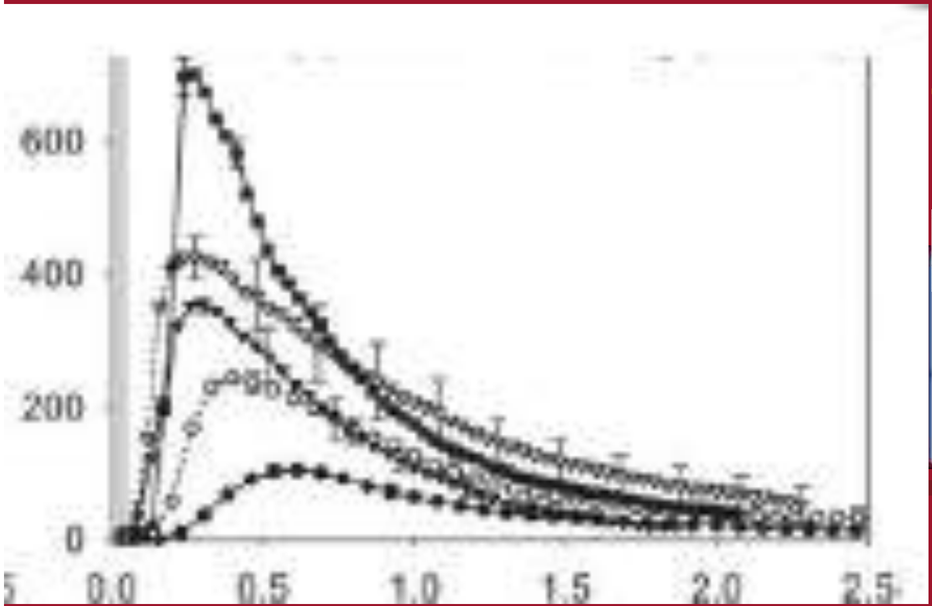

NIH $15.5M Transform. Grant

UC DAVIS UNIVERSITY OF CALIFORNIA

Penn University of Pennsylvania

Berkeley Lab

From http://explorer.ucdavis.edu/

EXPLORER Consortium Selects Industry Partners

January 2017

UC Davis Received EXPLORER Mock-up System from UIH America

UNITED IMAGING

sensL sense light

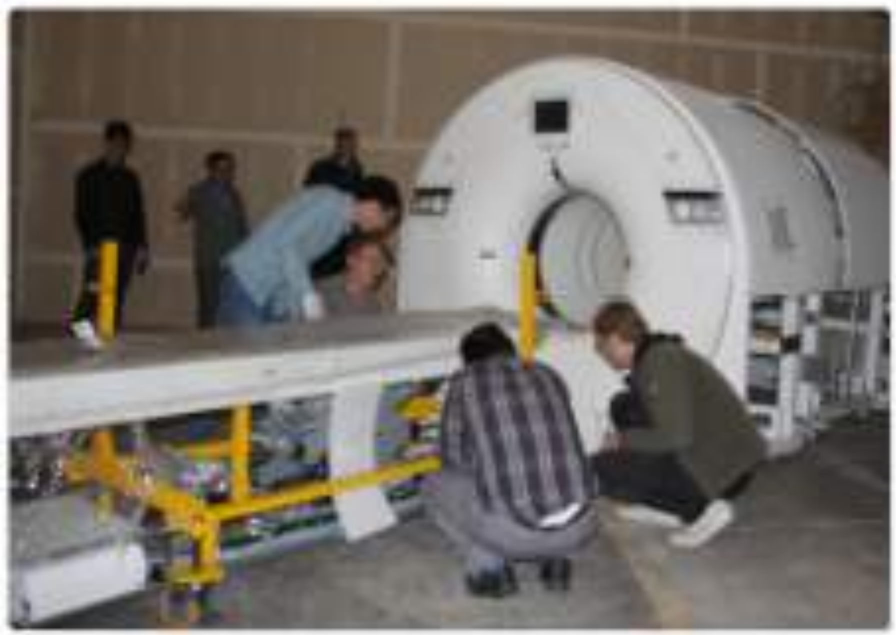

From http://explorer.ucdavis.edu/

THE UNIVERSITY OF CHICAGO BIOLOGICAL SCIENCES

EXPLORER: Total Body PET

- **Systemic disease and therapies:**
  - Cancer: Ultra-staging and micrometastasis
  - Inflammation
  - Infection
  - Cellular therapy and trafficking
  - Mind-body interactions
- **Total body pharmacokinetics**
  - Drug development
  - Toxicology
  - Biomarker discovery
- **Low Dose may enable:**
  - Expanded use in pediatrics
  - Use in chronic disease
  - Studies of normal biology

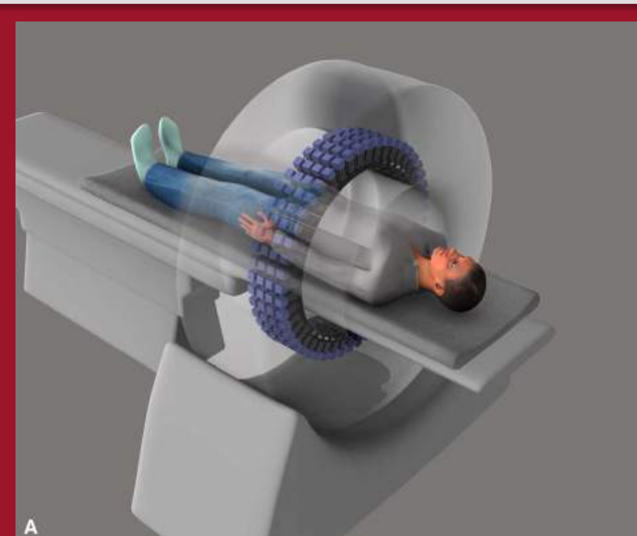

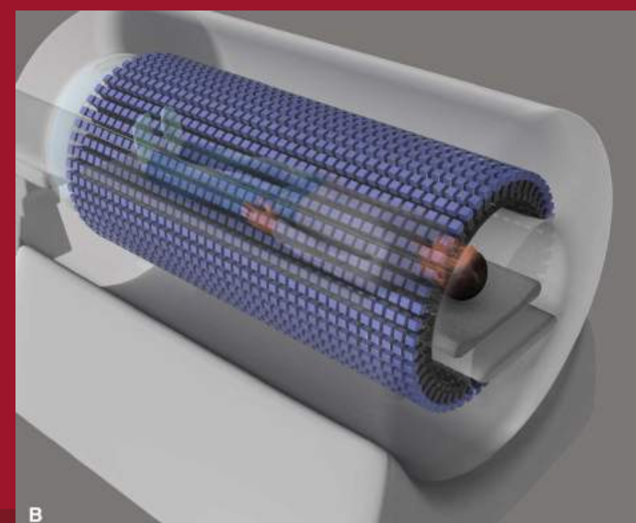

From http://explorer.ucdavis.edu/

Application-Specific Imaging Systems

PEM
Naviscan

NeuroPET/CT
Photon Diagnostic System Inc.
(PDSI)

GE Molecular Breast Imaging (MBI)

Newsoft Cardiac PET

Theranostic Use of MIBG in Neuroblastoma

Cohn/Vochenbaum (Pediatrics) &
Appelbaum/Pu/Armato/O'Brien-Penney/Chen (Radiology)

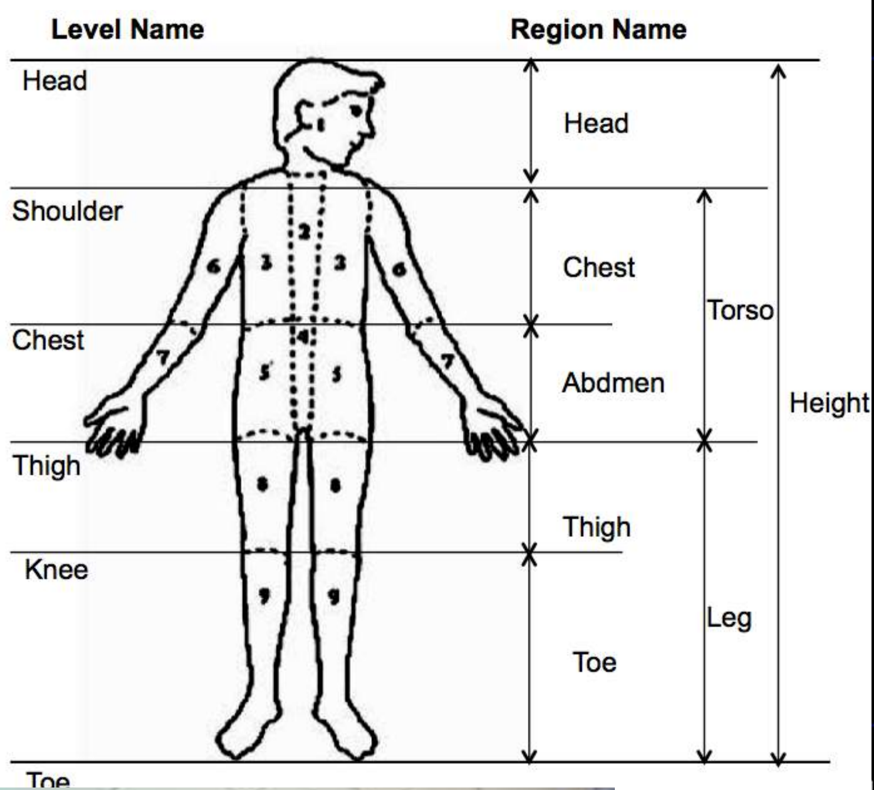

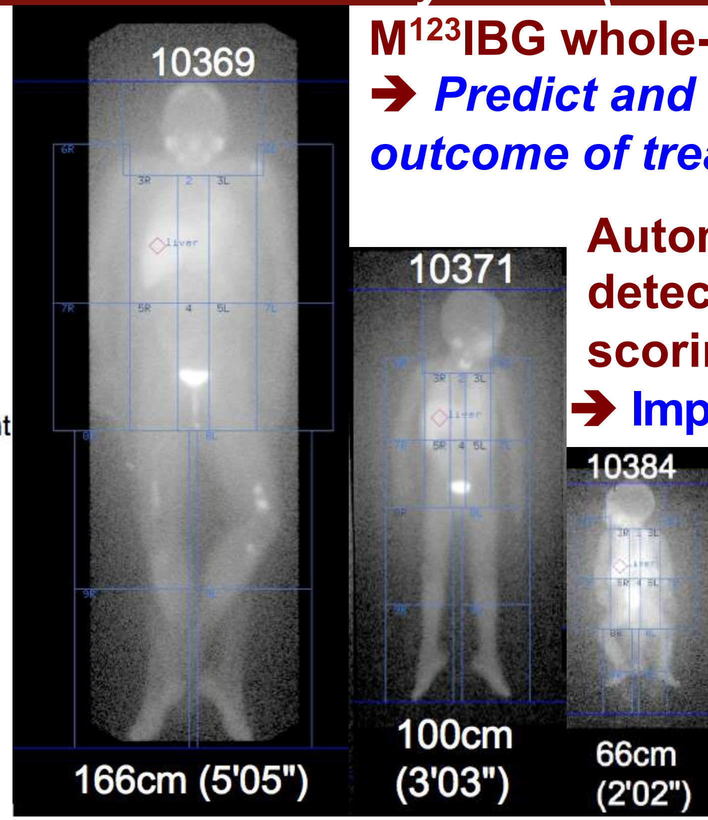

M^{123}IBG whole-body Imaging
➔ ***Predict and monitor the outcome of treatments***

Automated detection & scoring of lesions
➔ **Improved reliability**

computer-aided image analysis
➔ **Very challenging**

M^{131}IBG therapy trial ➔ High-risk NB patients
ANL/ATLAS-produced At-211 ➔ MABG therapy

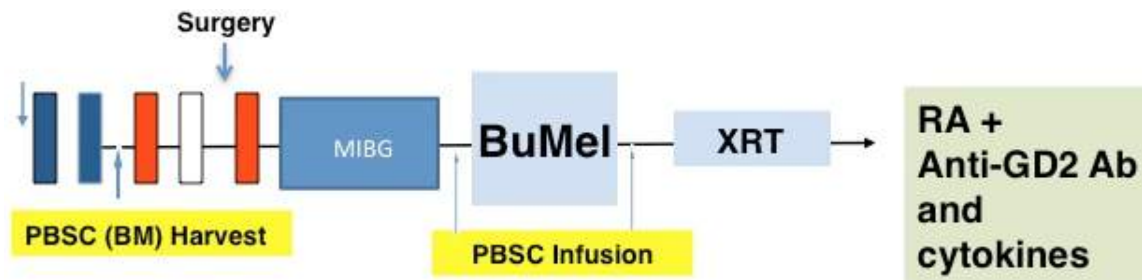

I-131: Beta-Decay; At-211: Alpha-Decay

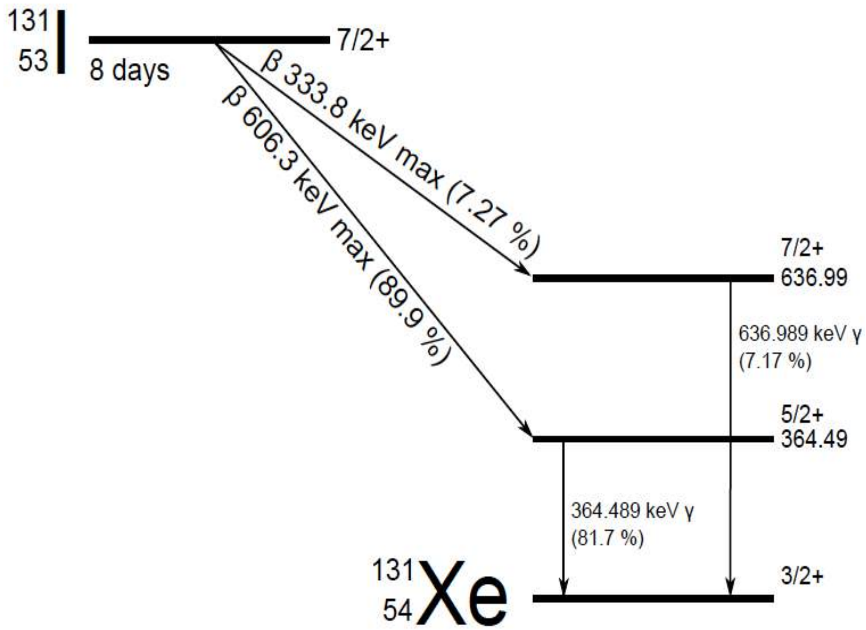

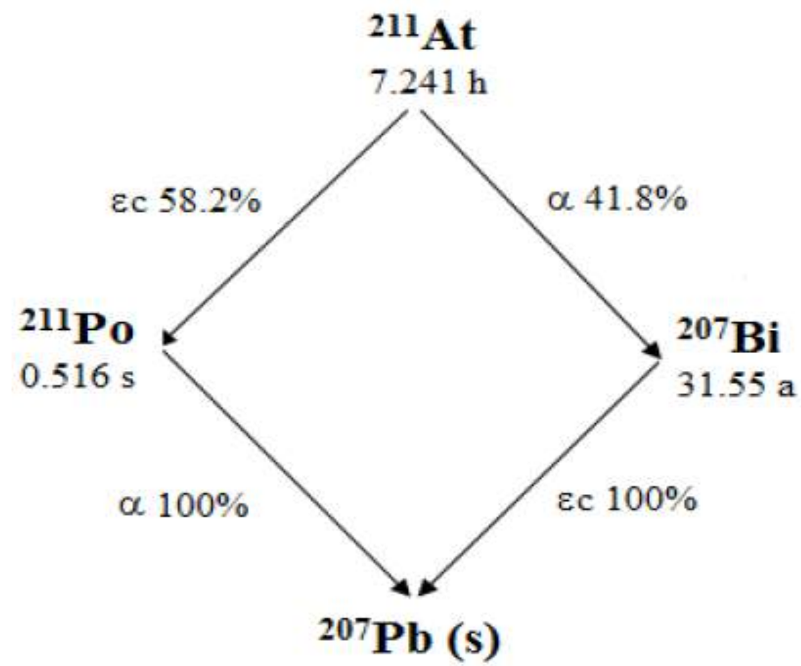

Mean Range:

I-131 β - ~ 40 cells **At-211 α - ~ 3 cells**

***Potential MABG Advantages*:**
- ***High Biological Effect***
- ***Lower Dose Delivery***
- ***Easier Safety Protection***

Argonne Superconducting Heavy Ion Linac

- Delivers any ion beam from protons to uranium
- Operates ~6000 hours per year

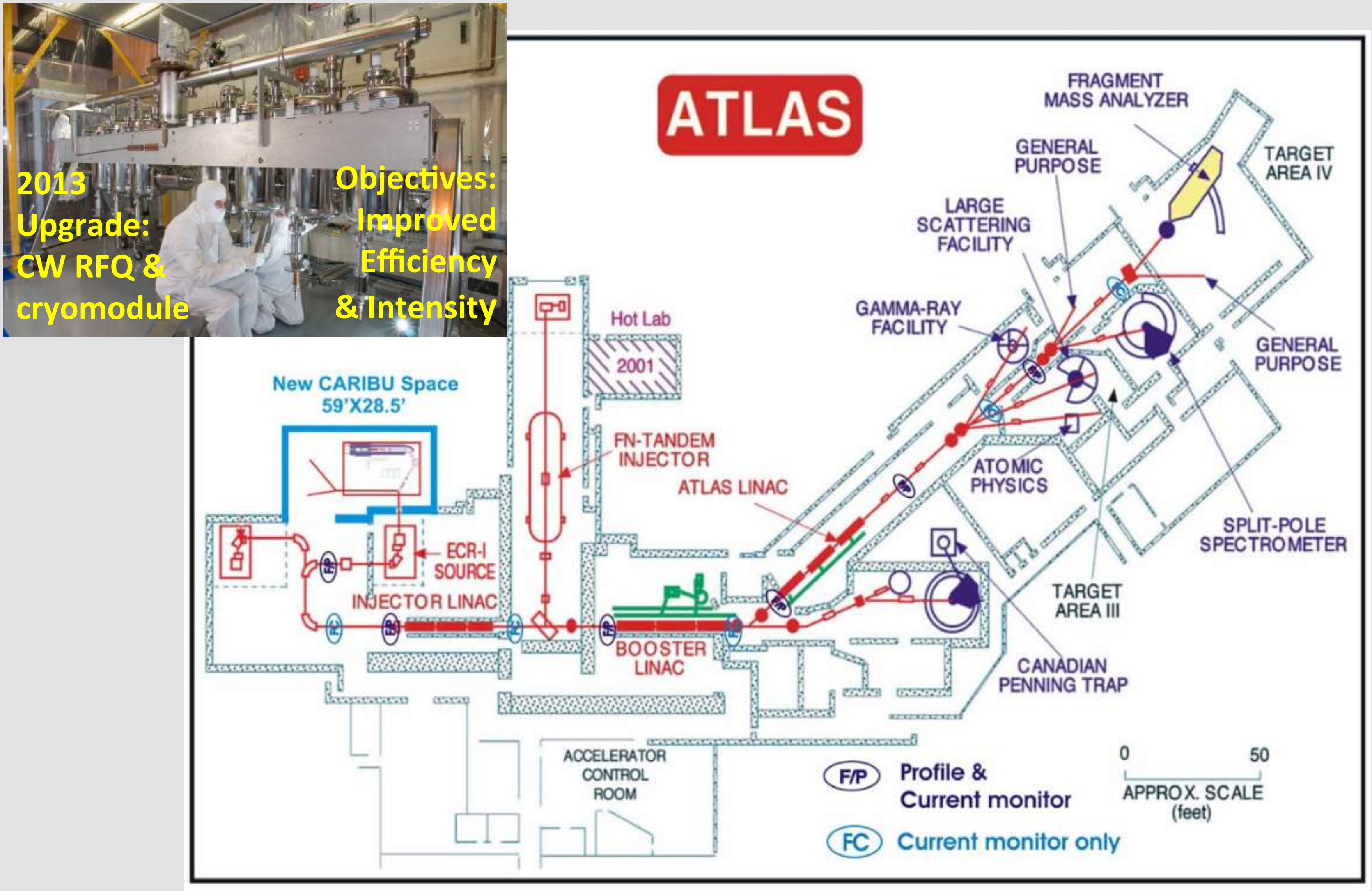

Addressing the Impracticality of ^{211}At

Short Half Life (7.2 h) & Extremely Limited Supply

- Only 4 production sites in the entire USA
- For SPECT Imaging, 13.2 h $t_{1/2}$ ^{123}I is commercially viable and supplied from limited production sites
- <u>Benchmark</u>: ^{211}At would be more attractive if $t_{1/2} \geq$ ^{123}I

^{211}**Rn** —14.6 h→ ^{211}**At**

Generator

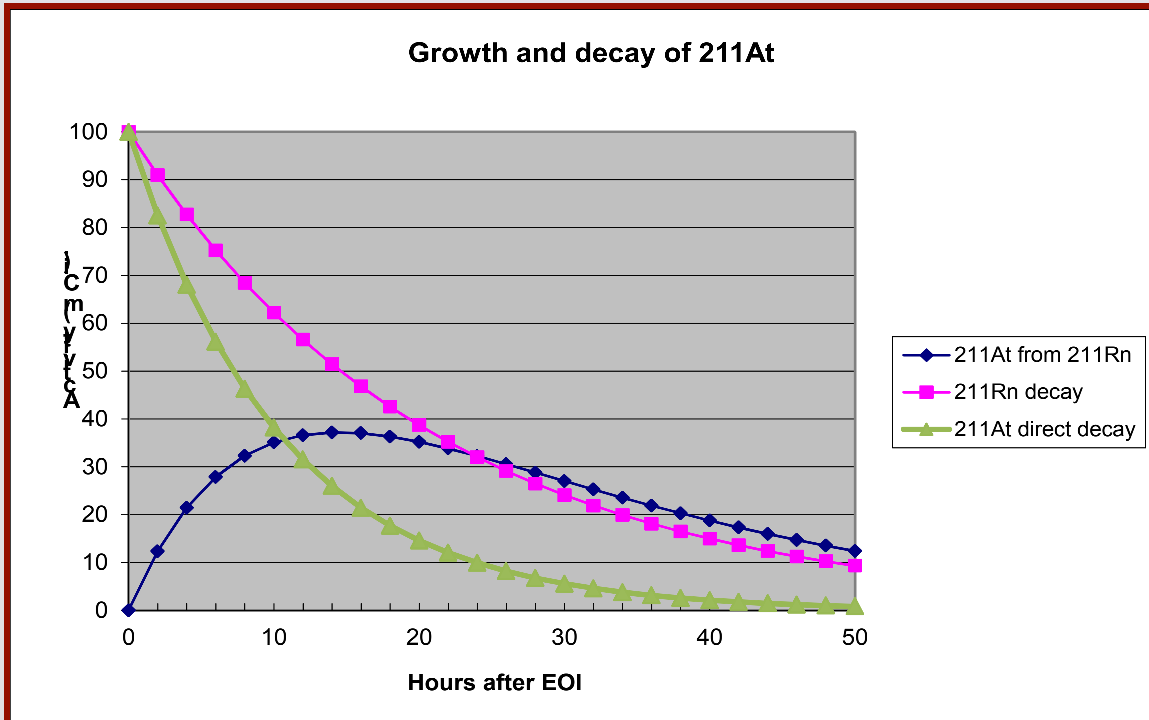

On-Board, In-Beam, In-Room CT, PET or SPECT for Radiation & Particle Therapy (Theranostics)

On-Board PET or SPECT

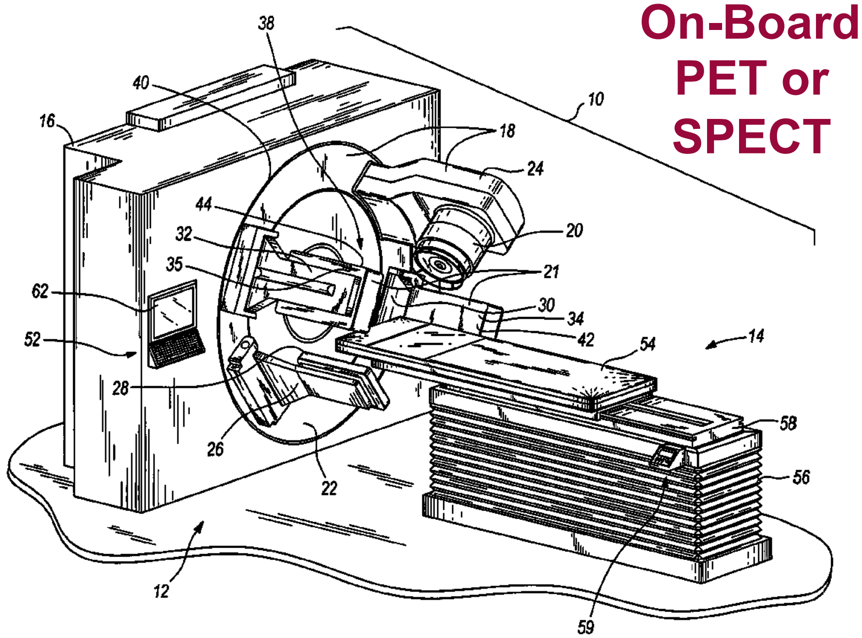

U.S. Patent No. 7,265,356 UCHicago

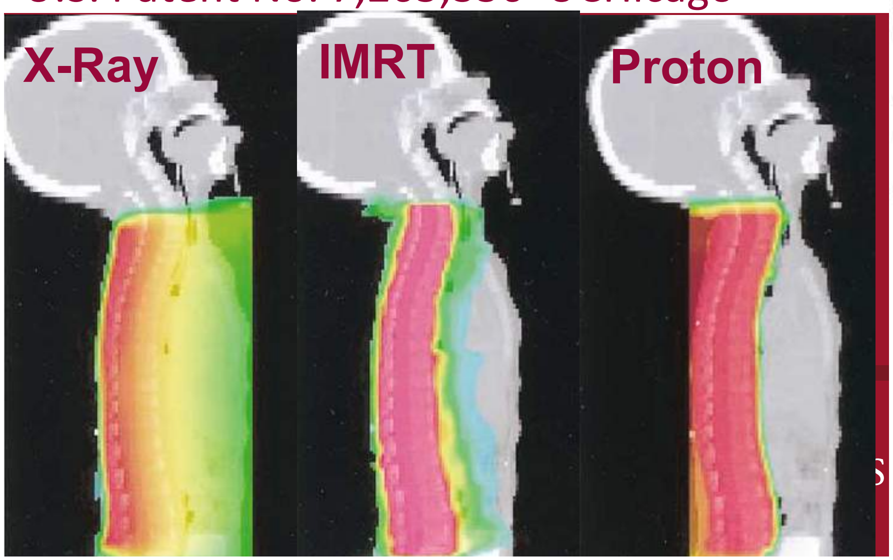

In-Beam **In-Room**

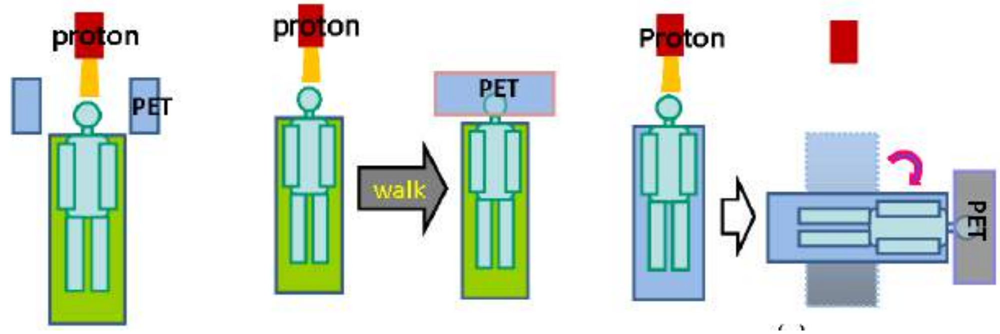

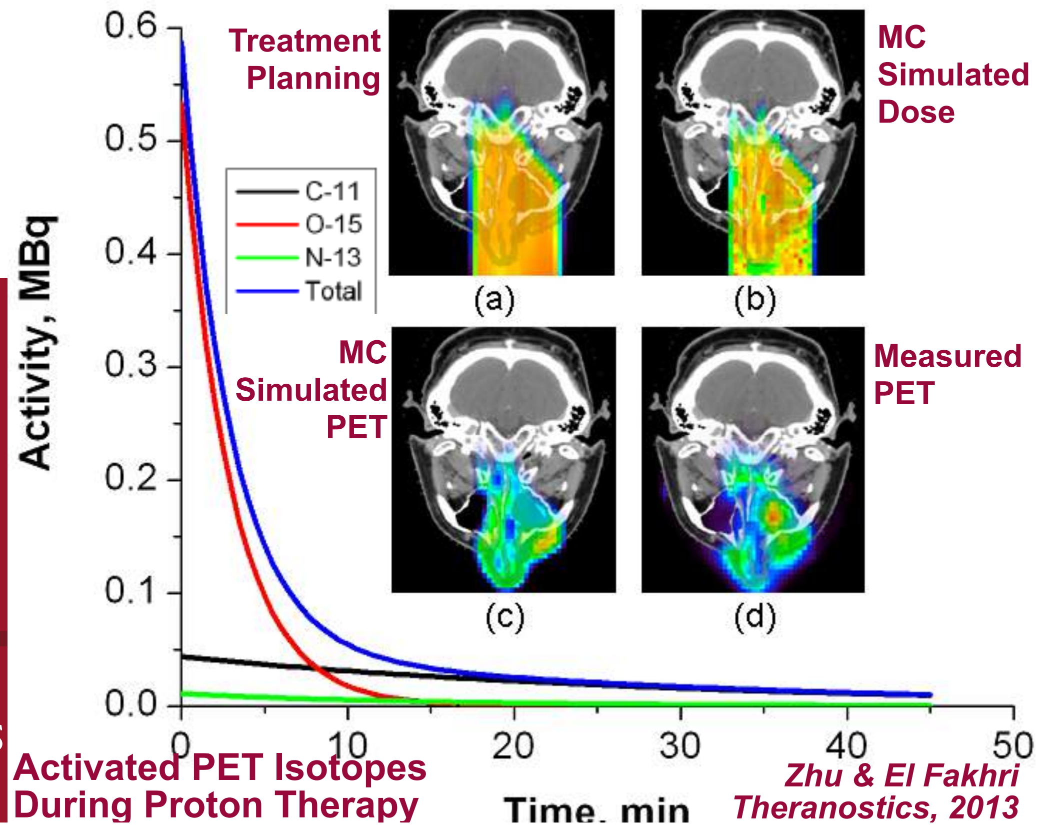

Activated PET Isotopes During Proton Therapy

Zhu & El Fakhri Theranostics, 2013

Summary

Crescat scientia; vita excolatur

Future Applications of TIPP in Medical Imaging

"Let knowledge grow from more to more, and so be human life enriched"

厚益生智

Technology and Instrumentation are in need to enable and/or improve the following:

(1) Multi-Modality Imaging
(2) Quantitative Imaging
(3) Modular and Transformable Imaging Devices
(4) Application-Specific Imaging Systems
(5) Theronostic Uses: Imaging and Image-Guided Therapy
(6) Synergistic and Holistic Integration with Imaging Chemistry, Computing, and Data Science